

Online Research @ Cardiff

This is an Open Access document downloaded from ORCA, Cardiff University's institutional repository: <https://orca.cardiff.ac.uk/id/eprint/134770/>

This is the author's version of a work that was submitted to / accepted for publication.

Citation for final published version:

Li, Wenjun, Shao, Longyi, Wang, Wenhua, Li, Hong, Wang, Xinming, Li, Yaowei, Li, Weijun, Jones, Tim ORCID: <https://orcid.org/0000-0002-4466-1260> and Zhang, Daizhou 2020. Air quality improvement in response to intensified control strategies in Beijing during 2013–2019. *Science of the Total Environment* 744 , 140776. 10.1016/j.scitotenv.2020.140776 file

Publishers page: <http://dx.doi.org/10.1016/j.scitotenv.2020.140776>
<<http://dx.doi.org/10.1016/j.scitotenv.2020.140776>>

Please note:

Changes made as a result of publishing processes such as copy-editing, formatting and page numbers may not be reflected in this version. For the definitive version of this publication, please refer to the published source. You are advised to consult the publisher's version if you wish to cite this paper.

This version is being made available in accordance with publisher policies.

See

<http://orca.cf.ac.uk/policies.html> for usage policies. Copyright and moral rights for publications made available in ORCA are retained by the copyright holders.



Air quality improvement in response to intensified control strategies in Beijing during 2013–2019

Wenjun Li^a, Longyi Shao^{a,*}, Wenhua Wang^a, Hong Li^b, Xinming Wang^c, Yaowei Li^a, Weijun Li^d,
Tim Jones^e, Daizhou Zhang^f

^a College of Geoscience and Surveying Engineering, China University of Mining and Technology (Beijing), Beijing 100083, China

^b State Key Laboratory of Environmental Criteria and Risk Assessment, Chinese Research Academy of Environmental Sciences, Beijing 100012, China

^c State Key Laboratory of Organic Geochemistry and Guangdong Key Laboratory of Environmental Protection and Resources Utilization, Guangzhou Institute of Geochemistry, Chinese Academy of Sciences, Guangzhou 510640, China

^d Department of Atmospheric Sciences, School of Earth Sciences, Zhejiang University, Hangzhou 310027, China

^e School of Earth and Ocean Sciences, Cardiff University, Museum Avenue, Cardiff, CF10, 3YE, UK

^f Faculty of Environmental and Symbiotic Sciences, Prefectural University of Kumamoto, Kumamoto 862-8502, Japan

First Author: Wenjun Li, (1992-), Ph. D candidate. Email: liwenjun_620@126.com

* Corresponding author: Longyi Shao, (1964-). Email: shaol@cumtb.edu.cn. Full postal address: No. 11, Xueyuan Rd., Haidian District, Beijing, P. R. China, 100083.

Highlights:

1. The air quality of Beijing before and after two action plans was assessed.
2. SO₂ decreased the most, followed by CO, PM_{2.5}, PM₁₀, and NO₂, while O₃ increased slightly.
3. The control of coal consumption played a dominant role in pollutant reduction.
4. The influences from meteorology, pollutant emissions, and energy structure were evaluated.
5. The control measures have proved to be effective in improving Beijing's air quality.

40 **Abstract**

41 The air pollution in Beijing has become of increasing concern in recent years. The
42 central and municipal governments have issued a series of laws, regulations, and
43 strategies to improve ambient air quality. The "Clean Air Action" and the
44 "Comprehensive Action" implemented during 2013–2017 largely addressed this
45 concern. In this study, we assessed the effectiveness of the two action plans by
46 environmental monitoring data and evaluated the influencing factors including
47 meteorology, pollutant emissions, and energy structure. The spatial distributions of air
48 pollutants were analyzed using the Kriging interpolation method. The Principal
49 Component Analysis-Multiple Nonlinear Regression (PCA-MNLR) model was applied
50 to estimate the effects of meteorological factors. The results have shown that Beijing's
51 air quality had a measurable improvement over 2013–2019. "Good air quality" days
52 had the highest increases, and "hazardous air quality" days had the most decreases. The
53 concentration of SO₂ decreased most, followed by CO, PM_{2.5}, PM₁₀, and NO₂ in
54 descending order, but O₃ showed a fluctuant increase. The "Comprehensive Action"
55 was more effective than the "Clean Air Action" in reducing heavy pollution days during
56 the heating period. The meteorological normalized values of the main pollutants were
57 lower than the observation data during 2013–2016. However, the observed values
58 became lower than the normalized values after 2017, which indicated beneficial
59 weather conditions in 2017 and afterwards. The emissions of SO₂ and dust significantly
60 decreased while NO_x had a slight decrease, and the energy structure changed with a
61 dramatic decrease in coal consumption and an obvious increase in the use of natural gas
62 and electricity. The significant reduction of coal-fired emissions played a dominant role
63 in improving Beijing's air quality, and vehicle emission control should be further
64 enhanced. The results demonstrated the effectiveness of the two action plans and the
65 experience in Beijing should have potential implications for other areas and nations
66 suffering from severe air pollution.

67 **Keywords:** Air quality, Clean Air Action, Comprehensive Action, effectiveness
68 evaluation, PCA-MNLR model, Beijing

69 **1. Introduction**

70 In recent decades, China has achieved rapid industrialization and urbanization. As
71 a result, severe air pollution problems appeared and became a major concern in China,
72 especially in Beijing (Wang et al., 2018b; Zhang, 2019; Li et al., 2019b; Xu and Zhang,
73 2020). Air pollution has generated great public concern due to its influence on
74 atmospheric visibility, human health, and global climate change (Sheehan et al., 2016;
75 Huang et al., 2018; Wang et al., 2019c; Liu et al., 2020). To alleviate air pollution, the
76 Beijing Municipal Government (BMG) formulated a series of control policies, laws,
77 and regulations that focused most on SO₂ and total suspended particulate (TSP) control
78 since 1998 (Wang et al., 2008; Zhang et al., 2016). However, the severe haze episodes
79 still occurred, especially in the heating seasons (autumn and winter). One of these
80 severe pollution episodes happened in January 2013, when the monthly average
81 concentration of PM_{2.5} reached almost 160 µg/m³, affecting about 1.3 million km² and
82 800 million people in northern China (Huang et al., 2014; Li et al., 2015).

83 Since then, the State Council of China issued the "Air Pollution Prevention and
84 Control Action Plan" (shorten to the APPCAP) on September 10, 2013 (The State
85 Council of China, 2013). The APPCAP is the first national strategy targeting PM_{2.5}
86 pollution and air quality improvement in China by setting specific quantitative targets
87 and clear time nodes (Feng et al., 2019). In particular, as a key city, the PM_{2.5}
88 concentration of Beijing should be kept below 60 µg/m³ by 2017. To fulfill the target,
89 Beijing has made further efforts according to the guidance of the APPCAP. The BMG
90 issued its own "Beijing 2013–2017 Clean Air Action Plan" (the Clean Air Action) in
91 September 2013 (BMG, 2013), which implemented much more stringent control
92 measures than ever before. However, heavy pollution days still occurred frequently in
93 the winter of 2016 (Wang et al., 2018a). To accomplish the five-year target the "Action
94 Plan for Comprehensive Control of Atmospheric Pollution in Autumn and Winter of
95 Beijing-Tianjin-Hebei region in 2017–2018" (the Comprehensive Action) was carried
96 out subsequently in autumn 2017 (MEP, 2017). The control measures on coal-fired
97 emissions were enhanced in the heating seasons (generally from 15th November to 15th

98 March of the next year). By the end of 2017, the annual mean concentration of PM_{2.5}
99 reduced to 58 µg/m³ from 89.5 µg/m³ in 2013, which fully achieved the five-year goal
100 of the Clean Air Action (Beijing Environment Statement, 2017). Thereafter, the State
101 Council issued a three-year plan on defending the blue sky during 2018–2020. The
102 "Action Plan for Comprehensive Control of Atmospheric Pollution in Autumn and
103 Winter of Beijing-Tianjin-Hebei region" was annually released both in Beijing and its
104 surrounding areas. The annual mean concentration of PM_{2.5} has decreased to 51 µg/m³
105 in 2018 and 42 µg/m³ in 2019, indicating that Beijing's air quality has improved yearly
106 (Beijing Ecology and Environment Statement, 2019).

107 Analysis of the air pollution characteristics of Beijing and its prominent air
108 pollution control approach after the Clean Air Action can provide valuable guidance in
109 optimizing control measures for policymakers. A significant body of research has
110 shown that pollutant emission controls played a dominant role in the decrease of PM_{2.5}
111 and other pollutants (Zhang et al., 2019b), and the meteorological factors, secondary
112 formation, and regional transport from the surrounding area had a significant influence
113 as well (Cai et al., 2017; Cheng et al., 2019a; Zhang, 2019). A large number of studies
114 have evaluated the air quality improvement by air quality data from online monitoring
115 (Liang et al., 2016; Cui et al., 2019; Chang et al., 2019), offline ground observation (Ma
116 et al., 2017; Wang et al., 2019d; Yang et al., 2020), and remote sensing (Wu et al., 2016;
117 Li et al., 2019a; Geng et al., 2019). Chemical transport models, such as CAMx, WRF-
118 Chem, and WRF-CMAQ (Zhang et al., 2019a; Geng et al., 2019; Zhang et al., 2019b),
119 were frequently applied to analyze the intrinsic mechanism and influencing factors. Xue
120 et al. (2019) found the national population-weighted annual mean PM_{2.5} decreased by
121 32% in China during 2013–2017. Chen et al. (2019) found that the control of
122 anthropogenic emissions contributed to 80% of the decrease in PM_{2.5} concentration in
123 Beijing 2013–2017. Statistical models, such as the deep neural network model,
124 convergent cross-mapping (CCM) method, and the difference-in-difference (DID)
125 model are other methods to decouple the influencing factors such as meteorology,
126 pollutant emissions (Cobourn et al., 2010; Chen et al., 2018b; Wang et al., 2019a). Vu
127 et al. (2019) found the primary emission controls have led to reductions in PM_{2.5}, PM₁₀,

128 NO₂, SO₂, and CO of about 34%, 24%, 17%, 68%, and 33% during 2013–2017 in
129 Beijing, after meteorological correction.

130 Most of these studies were either concentrated on the long-term effect evaluation
131 of certain air pollutants or focused on the short-term for one season or one year period.
132 These studies could provide valuable insights into the effectiveness of the Clean Air
133 Action. However, the simulations usually have biases compared with ground
134 observations because of the uncertainties in the emission inventory and the missing
135 mechanisms in models, as well as the heavy workload and massive volume of multiple
136 data. Indeed, it is hard to measure the effectiveness of a policy due to compound factors
137 and inner mechanisms, and the relationships among multiple air pollutants are non-
138 linear related. Therefore, it is necessary to analyze both the spatio-temporal patterns of
139 air pollutants and the influencing factors.

140 In this study, we compared the effectiveness of the Clean Air Action and the
141 Comprehensive Action against the environmental monitoring data in Beijing during
142 2013–2019, and analyzed the influencing factors of meteorology, emission reduction,
143 and energy structure. The spatial distribution of six air pollutants in Beijing during
144 2013–2019 was analyzed by the Kriging interpolation method for the first time. The
145 PCA-MNLR model was applied to estimate the influences of meteorological factors. In
146 comparison with the previous researches, this is the first attempt to integrate
147 investigation of the spatio-temporal patterns of six types of air pollutants and the
148 quantitative simulation of the influencing factors over Beijing during 2013–2019. We
149 hope Beijing's experience could be beneficial for other megacities in the world suffering
150 from similar air pollution problems.

151 **2. Data and methods**

152 **2.1. Study area**

153 As the capital, political and cultural center of China, Beijing (39.13°–41.08° N and
154 115.22°–117.50° E) is located in the northwest part of the North China Plain,
155 surrounded by the northern Yanshan Mountains and the western Taihang Mountains
156 (Fig. 1). Beijing has a typical temperate and monsoonal climate with high humidity

157 summers and cold, windy, and dry winters. Moreover, Beijing covers a total provincial
158 area of 16,410 km² with a population of 21.5 million (BSY, 2019). The central urban
159 areas of Beijing include six districts, i. e. Haidian (HD), Chaoyang (CY), Dongcheng
160 (DC), Xicheng (XC), Fengtai (FT), and Shijingshan (STS).

161 **2.2. Data sources**

162 In this study, air quality data was obtained from the Beijing ambient air automatic
163 monitoring system. This system consists of 35 air monitoring stations, including 12
164 state-controlled stations and 23 city-controlled stations (Fig. 1). The real-time data are
165 released to the public by the Beijing municipal environmental monitoring center
166 (BMEMC) (<http://www.bjmemc.com.cn/>). The data was downloaded from the websites
167 (<https://github.com/tuanvvu> and <http://beijingair.sinaapp.com/#messy>), where the real-
168 time values are recorded. Data from the 35 monitoring stations included the hourly
169 value of air pollutants from January 17th, 2013 to February 29th, 2020, and air quality
170 index (AQI) from January 1st, 2014 to February 29th, 2020. The air pollutants consisted
171 of PM_{2.5}, PM₁₀, SO₂, NO₂, CO, and O₃. These pollutants are measured by the Thermo
172 Fisher instrument series, which are calibrated by standard gases every two days (Wang
173 et al., 2015). The measurement method and instrument for each pollutant are shown in
174 Table S1. On the other hand, AQI is a comprehensive index calculated by considering
175 six major pollutants, which could reflect the overall air quality (Zhan et al., 2018; Tian
176 et al., 2019).

177 The pollutant emission data included the annual mean concentration of SO₂, NO_x,
178 and dust emissions. The socio-economic data included the annual mean of the
179 permanent population, total energy consumption, gross domestic product (GDP), and
180 vehicle numbers. The energy structure data included the annual means of coal,
181 petroleum, natural gas, and electricity consumption (BSY, 2019). Hourly
182 meteorological data including temperature, relative humidity (RH), wind speed (WS),
183 atmospheric pressure (AP), and visibility (VIS) from January 1st, 2013 to February
184 29th, 2020, and were downloaded from the website (<http://hz.zc12369.com/home/>).

185 2.3. Data analysis

186 We calculated the AQI daily mean values in 2013 by Eq. (1) and Eq. (2) according
187 to the technical regulations on ambient air quality index (HJ633–2012). The individual
188 air quality index (IAQI) is the air quality index of each air pollutant. AQI and IAQI are
189 dimensionless indexes. The corresponding threshold of each pollutant was presented in
190 Table 1.

$$191 \quad IAQI_p = \frac{IAQI_{Hi} - IAQI_{Lo}}{BP_{Hi} - BP_{Lo}} (C_p - BP_{Lo}) + IAQI_{Lo} \quad \text{Eq. (1)}$$

$$192 \quad AQI = \max\{IAQI_1, IAQI_2, IAQI_3, \dots, IAQI_6\} \quad \text{Eq. (2)}$$

193 where $IAQI_p$ is the index for pollutant p , C_p is the concentration of pollutant p ,
194 BP_{Hi}/BP_{Lo} is the breakpoint that is greater/less than or equal to C_p , $IAQI_{Hi}/IAQI_{Lo}$ is the
195 AQI value corresponding to BP_{Hi}/BP_{Lo} . The maximum of the $IAQI$ is defined by the
196 value of AQI.

197 Depend on the different extent of human health impacts regulated by Table 2
198 according to the technical regulations on ambient air quality index (HJ633–2012), AQI
199 is subdivided to different levels of air quality, including the levels of good (AQI: 0–50),
200 moderate (AQI: 51–100), unhealthy for sensitive groups (AQI: 100–150), unhealthy
201 (AQI: 150–200), very unhealthy (AQI: 200–300), and hazardous (AQI: >300).

202 The daily average, monthly average, seasonal average, and the annual average of
203 air pollutant concentration and AQI were calculated by the arithmetic mean method.
204 The average of 12 state-controlled stations was used to represent the overall air quality
205 of Beijing. The daily average value was obtained by averaging hourly data from 00:00
206 to 23:00. As some data were missing due to instrument failure or internet error, and
207 some data were considered abnormal, observation for at least 20 hours is required to
208 obtain a daily average concentration of each pollutant for each station. Moreover, at
209 least 27 days and 324 days are required to obtain monthly and annual average
210 concentration, respectively. Otherwise, the invalid data was excluded. All calculations
211 were carried out according to the National Ambient Air Quality Standards (GB3095–
212 2012) (Table 3), technical regulations on ambient air quality index (HJ633–2012)

213 (http://www.gov.cn/zwggk/2012-03/02/content_2081374.htm), and technical
214 regulations for ambient air quality assessment (HJ663–2013)
215 (http://www.mee.gov.cn/ywgz/fgbz/bz/bzwb/jcffbz/201309/t20130925_260809.shtml).

216 The concentrations of air pollutants have strong spatial self-aggregation effects,
217 which proved the necessity for regional integration of air quality management (Chen et
218 al., 2019b). For Beijing, the geographical location, land use, and types of the functional
219 zones for monitoring stations are different. To obtain spatial variations of air pollutants
220 in Beijing, we employed geographic information system (GIS) which could facilitate
221 the understanding at spatial perspectives, and conducted the Kriging interpolation
222 method which is a typical statistical algorithm widely applied in geoscience and
223 atmospheric science (Liu et al., 2017; Hu et al., 2019). We applied the Kriging method
224 using ArcGIS 10.2 software to investigate the spatial distribution of air pollutants from
225 35 monitoring stations in Beijing.

226 **2.4. PCA-MNLR method**

227 In this study, a multiple nonlinear regression (MNLR) method was employed to
228 analyze the relationship between meteorological variables; namely temperature,
229 relative humidity (RH), wind speed (WS), atmospheric pressure (AP), and visibility
230 (VIS), and six air pollutant concentrations variables; namely PM_{2.5}, PM₁₀, SO₂, NO₂,
231 CO, and O₃. The regression model requires a low correlation between variables,
232 otherwise, the multicollinearity will affect the accuracy of the simulation results. Thus,
233 the Principal Component Analysis (PCA) method was used to find patterns in data of
234 high dimension by reducing the dimensionality (Salim et al., 2019; Li et al., 2018). As
235 a simple, quick, and accurate statistical method, the Principal Component Analysis-
236 Multiple Nonlinear Regression (PCA-MNLR) method, or named principal components
237 regression (PCR), was employed by using the MATLAB R2019b software (MathWorks,
238 Natick, MA, USA). PCA-MNLR method has been applied for predicting air pollution
239 by several studies (Tan et al., 2016; Li et al., 2018).

240 The meteorological factors were set as independent variables, and the air pollutant
241 concentrations were set as dependent variables. Firstly, the described data dependency

242 by Eq. (3) found strong correlations in most of the dependent variables. Due to the
 243 complex natural environment, there are different dimensions between environmental
 244 data, such as PM_{2.5} (μg/m³) and temperature (°C). Data were firstly nondimensionalized
 245 into proper dimensionless indexes by the Eq. (4).

$$246 \quad R(X, Y) = \frac{\sum_{i=0}^n (x_i - \bar{x})(y_i - \bar{y})}{\sqrt{\sum_{i=0}^n (x_i - \bar{x})^2} \sqrt{\sum_{i=0}^n (y_i - \bar{y})^2}} \quad \text{Eq. (3)}$$

$$247 \quad z_{ij} = \frac{x_{ij} - \min(x_{ij})}{\max(x_{ij}) - \min(x_{ij})} \quad \text{Eq. (4)}$$

248 In Eq. (3), where $R(X, Y)$ represents the correlation coefficient between two dependent
 249 variables. The closer of $|R(X, Y)|$ to 1, the more correlative between X and Y , and the
 250 nearer to 0, the more unobvious correlative between X and Y . In Eq. (4), where i is the
 251 year, j is the number index, x_{ij} is the data of j index in i year, $\min(x_{ij})$ is the minimum
 252 value of j th index, and $\max(x_{ij})$ is the maximum value of j th index.

253 The above data was principal component transformed to get the eigenvector matrix
 254 Coeff, the score matrix Score (Y), and the eigenvalue matrix latent. After the PCA
 255 process, the correlations in dependent variables were checked again. Due to the
 256 nonlinear relationship between the influencing factors, a power function was employed
 257 to perform the multivariate non-linear regression analysis by Eq. (5), and the natural
 258 logarithm of both sides of Eq. (5) were taken by Eq. (6).

$$259 \quad y = \alpha_0 X_1^{\alpha_1} X_2^{\alpha_2} \dots X_k^{\alpha_k} \quad \text{Eq. (5)}$$

$$260 \quad \ln(y) = a_0 + a_1 \ln X_1 + a_2 \ln X_2 + \dots + a_k \ln X_k \quad \text{Eq. (6)}$$

261 **2.5. Control measures**

262 Based on nearly 20 years of air pollution control, China has issued a series of strong
 263 air pollution prevention and control programs and ultimately developed a rich
 264 experience in air quality management (UN Environment, 2019). In the APPCAP, as a
 265 milestone, the control pollutants changed from the traditional pollutants (SO₂, NO_x,
 266 smoke, and dust) to multiple pollutants including SO₂, NO_x, primary particulate matter,
 267 and volatile organic compounds (VOCs). Non-point source pollution controls had been

268 greatly strengthened instead of the previous industrial point sources. The key control
269 regions included the Beijing-Tianjin-Hebei (BTH) area, the Yangtze River Delta (YRD),
270 and the Pearl River Delta (PRD). The APPCAP is for nationwide control while the
271 Clean Air Action is set by Beijing for the local emissions control. Particularly, as the
272 principal action plans for Beijing, the Clean Air Action emphasized the integrated
273 control measures, and the Comprehensive Action focused on the coal-fired emission
274 reductions in autumn and winter that played a dominant role in its air quality
275 improvement during 2013–2019. These measures greatly reduced coal-fired emissions.
276 The major control measures of these two action plans are given in Table 4.

277 **3. Results**

278 **3.1. Trends of AQI**

279 During 2013–2019, the overall air quality in Beijing has improved dramatically,
280 with the annual mean AQI decreasing year by year (Fig. 2). The proportion of meeting-
281 standard days (AQI < 100) increased from 48.4% to 66.8%, and heavy pollution days
282 (AQI > 200) decreased from 15.4% to 1.1%. During these seven years, the number of
283 good air quality days had the most significant increase (111.7%), followed by moderate
284 air quality days (16.9%) and unhealthy for sensitive (5.8%) in descending order. In
285 association with these increases, hazardous days had the greatest decrease, falling from
286 14 days to zero, followed by very unhealthy days (90.6%) and the unhealthy days
287 (40.7%).

288 Fig. 3 shows the time-series of the daily average of AQI. In northern China, heavy
289 pollution days mostly happen in autumn and winter due to the central heating (Qiu et
290 al., 2017). After the Clean Air Action implemented in 2013, the heavy air pollution days
291 decreased in spring (4.1%), summer (70%), and autumn (6.6%) during 2013–2016,
292 while the heavy air pollution days increased by 44.8% in winter. After the stringent
293 control measures of the Comprehensive Plan implemented in autumn 2017, the daily
294 value of AQI had a dramatic decrease (shown by the red circles in Fig. 3). During 2016–
295 2017, heavy pollution days dramatically decreased by 88% in winter and 78.6% in
296 autumn, and the meeting-standard days increased by 57.0% in winter and 32.4% in

297 autumn. Therefore, compared to the Clean Air Action, the Comprehensive Action is
298 more effective in reducing the heavy pollution days in the heating seasons.

299 **3.2. Trends of air pollutants**

300 Between 2013 and 2019, the annual mean concentration of PM_{2.5}, PM₁₀, SO₂, NO₂,
301 and CO decreased by 53.1%, 37.1%, 84.9%, 33.9%, and 58.8%, respectively, while O₃
302 slightly increased by 4.1% in Beijing (Table 5). During the past seven years, SO₂ had
303 the greatest decrease, followed by CO, PM_{2.5}, PM₁₀, and NO₂ in descending order.
304 However, O₃ increased in 2013–2015 and then decreased after 2016; the annual average
305 of O₃ in 2019 was still higher than in 2013. Compared to the National Ambient Air
306 Quality Standard II, the annual mean concentrations of SO₂ and CO in 2019 were much
307 lower than the standard, and NO₂ and PM₁₀ were 7.5% and 2.9% lower than the
308 standard, which was the first time the standard was reached in recent years. However,
309 PM_{2.5} and O₃ were still 20.0% and 19.4% higher than the standard, respectively. In
310 conclusion, under the implementation of the Clean Air Action and the Comprehensive
311 Action from 2013 to 2019, the reductions of SO₂ and CO were very significant, but a
312 complicated type of compound PM_{2.5} and O₃ pollution emerged (Jin et al., 2016).

313 Fig. 4 shows the trends in the daily average, monthly average, and seasonal average
314 of air pollutants. The concentrations of PM_{2.5} were higher in autumn and winter than in
315 spring and summer. The seasonal distributions of PM₁₀, SO₂, NO₂, and CO were
316 approximately similar to PM_{2.5}. Typically, air pollution is worse in autumn and winter,
317 while air quality is relatively better in summer over this region (Zhang et al., 2018).
318 Thus, the seasonal characteristics of PM_{2.5}, PM₁₀, SO₂, NO₂, and CO showed a single
319 valley distribution with the minimum appeared in summer. However, O₃ had a different
320 seasonal variation compared to other pollutants, with higher concentrations in summer
321 and spring, and lower concentrations in autumn and winter, which often showed as a
322 single peak distribution with the maximum appeared in summer. The concentration of
323 SO₂ and CO decreased significantly in autumn and winter, which were close to the
324 values in spring and summer, so the trend in the seasonal distributions of SO₂ and CO
325 tended to be flat. However, the trends in PM_{2.5}, PM₁₀, NO₂, and O₃ still fluctuated

326 throughout the whole year.

327 **3.3. Temporal and spatial distribution of air pollutants in heating and non-heating** 328 **periods**

329 Before the Clean Air Action, the heat supply in Beijing was mainly by coal-fired
330 boilers, and the coal consumption was usually higher in the heating period, which could
331 directly aggravate haze pollution. After the implementation of the Clean Air Action, the
332 clean energy alternatives such as coal-to-gas or coal-to-electricity gradually took over
333 the coal-fired boilers in the heating seasons (Xu and Ge, 2020). To compare the coal
334 consumption in the heating seasons of these two action plans, the research period was
335 divided into two stages, including stage I (between the Clean Air Action and the
336 Comprehensive Action) and stage II (after the Comprehensive Action).

337 At stage I, the concentrations of PM_{2.5}, PM₁₀, SO₂, CO, and NO₂ in the heating
338 period remained much higher than in the non-heating period, while these concentrations
339 significantly declined at stage II (Fig. 5). Compared to 2016, PM_{2.5}, PM₁₀, SO₂, CO,
340 and NO₂ in the heating period of 2017 had decreased by 48.5%, 39.4%, 47.7%, 46.3%,
341 and 29.7%, respectively (Fig. S1). Especially in 2017, PM_{2.5} and PM₁₀ in the heating
342 period were 10.3% and 17.0% lower than in the non-heating period (Fig. S1). These
343 decreases were substantially related to the changing levels of coal consumption in the
344 heating seasons after the implementation of the Comprehensive Action. Decreasing
345 emissions from the coal-burning section are the key factor to control pollution during
346 the heating season (Qiu et al., 2017). Unlike other pollutants, the concentrations of O₃
347 were much higher in the non-heating period. At stage II, O₃ even increased in both the
348 heating period and the non-heating period. In summary, haze pollutions dominated by
349 particulate matter were controlled effectively, especially in the heating seasons, but
350 photochemical pollutions dominated by O₃ became increasingly prominent.

351 The vehicle emissions are always higher in the central urban areas with high traffic
352 density, and have no seasonal variations, while the coal-fired emissions tend to display
353 a seasonal variation with higher concentrations in the heating period. As Fig. 6 shows,
354 the spatial distributions of coal-fired pollutants including PM_{2.5}, PM₁₀, SO₂, and CO

355 were similar. These pollutants had higher concentrations in the southern and central
356 urban areas and relatively lower concentrations in the northern regions, which is related
357 with the regional transportation from the southern areas of Beijing (Zheng et al., 2015;
358 Zhang et al., 2017). However, NO₂ and O₃ had different distribution patterns. The
359 serious NO₂ pollution in the heating period was related to the extra coal-fired emission
360 source from heat supply, while in the non-heating period the source of NO₂ mostly came
361 from vehicle emissions. At stage I, the concentrations of NO₂ were high in central urban
362 areas in the non-heating period, and then the high NO₂ regions became wider in the
363 heating period, with a distribution in the southern and central urban areas, which are
364 mainly due to the extra coal consumption for central heating. At stage II, the high NO₂
365 regions were still centered in the central urban areas with high traffic density, but
366 became much more constrained than stage I. This change was particularly obvious in
367 the heating period. Therefore, the decrease in NO₂ was mainly due to the reduction of
368 NO_x from coal-fired emissions in the heating seasons.

369 Unlike other pollutants, the concentrations of O₃ in the non-heating period were
370 higher than in the heating period. After the strict implementation of the Comprehensive
371 Plan, the concentrations of O₃ increased further, especially in central urban areas during
372 the non-heating period of stage II. In the lower atmosphere, O₃ is a secondary pollutant
373 formed by the photochemical reaction of its precursors including organics like methane,
374 volatile organic compounds (VOCs), and non-methane volatile organic compounds
375 (NMVOCs), CO, and NO_x. (Tao et al., 2016). To only focus on NO_x emission reduction
376 may not work or even aggravate O₃ pollution, VOCs-targeted control is a more practical
377 and feasible way (Wang et al., 2019b). However, the control of VOCs is difficult due
378 to its non-organizational emissions, and the relationships between O₃ and its precursors
379 are non-linear, making the control of O₃ more challenging. In addition, the
380 concentrations of O₃ were higher in the suburb areas than in the traffic-related central
381 urban areas. Affected by vehicle emissions, the high concentrations of NO and NO₂
382 promote the reaction of O₃ with NO ($O_3 + NO \rightarrow NO_2 + O_2$) that frequently happens
383 in the urban area in summer, which consumes ozone (Wang et al., 2014). There is also
384 the terrestrial vegetation cover that is also regarded as an important source of VOCs,

385 which could promote O₃ formation in the suburb areas and affect the distribution of O₃
386 (Maji et al., 2019).

387 **4. Discussion**

388 **4.1. Impact of meteorological conditions on air pollutants**

389 The concentrations of air pollutants are closely related to meteorological conditions
390 (Nguyen et al, 2019; Zhang et al., 2019c; Chen et al., 2018a). An important aspect in
391 assessing air quality improvement is to consider the impact of meteorology (Chen et al.,
392 2017; Vu et al., 2019). Beneficial weather conditions with stronger wind speed, higher
393 local mixing layer heights (MLHs) could favour the dispersion of pollutants, while
394 adverse weather conditions with higher relative humidity, lower wind speed, less
395 rainfall, and more inversions, could aggravate air pollution conditions (Xu et al., 2020).

396 The meteorological factors were estimated by the PCA-MNLR model. Fig. 7 shows
397 the time-series variation of the meteorological normalized concentrations and the
398 observed concentrations of air pollutants during 2013–2019 in Beijing. By comparing
399 the results of observation and simulation, it indicated that the PCA-MNLR model could
400 reproduce the temporal distribution of air pollutants relatively well (R^2 : 0.73–0.82). The
401 meteorological normalized values (red line) had regular variations, which were similar
402 to the observation results (black line). During 2013–2016, the meteorological
403 normalized values of SO₂ and CO were just lower than the observed values, which
404 indicated that the real meteorological condition was more significant and this could
405 aggravate the SO₂ and CO pollution. However, after the implementation of the
406 Comprehensive Plan, the meteorological normalized values of SO₂ were higher than
407 the observed values, and the simulation and observation values of CO were close. This
408 was mainly due to the more beneficial weather condition favoring the dispersion of air
409 pollutants. Furthermore, SO₂ and CO had the most significant decreases over the seven
410 years. Previous studies have indicated that, compared with 2013, the meteorological
411 conditions worsened in 2014 and 2015 and improved in 2016 and 2017 (Zhang et al.,
412 2019c). Thus, the beneficial weather conditions in 2017 and afterwards helped the
413 dispersion of pollutants and promoted air quality improvement.

414 However, this variation pattern was not so consistent with PM_{2.5} and PM₁₀. The
415 differences between the stimulation and observation values of the particles were not so
416 similar as the variation of meteorology. The influencing factors in the concentration of
417 PM_{2.5} and PM₁₀ are more complicated, and only considering the relationship between
418 several meteorological conditions and air pollutants is insufficient. Moreover, the
419 meteorological normalized O₃ and NO₂ concentrations were always lower than the
420 observation results, which were different compared to other pollutants. One of the
421 reasons is that the influence of the meteorological factor was different for O₃ and NO_x,
422 and the interactions between O₃/NO_x and other air pollutants were more complicated.
423 The different meteorological conditions could not completely explain the difference
424 between the observation and simulation values, as previous analyses had indicated that
425 the meteorology contributed about 12.1%–31% of the total PM_{2.5} reduction in Beijing
426 (Zhang et al., 2019c; Cheng et al., 2019a; Cheng et al., 2019b). Although the
427 meteorological conditions significantly influenced the concentration of air pollutants,
428 the dominant factor driving this decrease was still the emission reductions made by
429 strict control measures (Chen et al., 2019a).

430 In addition, we compared the annual mean concentrations of air pollutants after the
431 meteorological normalization by this study and other references in Table S2. Moreover,
432 the PCA-MNLR results and other WRF-CMAQ modeling results by Cheng et al.
433 (2019a) were compared by the monthly concentrations (Fig. 8). The correlation
434 coefficients between monthly values by PCA-MNLR model was 0.84, while it was 0.78
435 for the WRF-CMAQ study. The difference between the monthly observation and the
436 simulation values of PM_{2.5} ranged from 0.3% to 23% with an average 10.3% difference
437 by PCA-MNLR. In contrast, the deviation changed to 3%–33.6% with an average of
438 10.3% for the WRF-CMAQ study.

439 Fig. 9 shows the score plot of the two principal components. The score plot could
440 help to elucidate the distribution of the observations and reveal the relative relationship
441 between data points. Theoretically, on the score plot, closer distribution means similar
442 behavior between samples (Camacho, 2014). In Fig. 9, each point represented the score
443 status of each day considering both the meteorological factors and air pollutant

444 concentrations. During 2013–2016, the daily meteorological normalized values of some
445 days in autumn and winter were still high (the high x-axis value in Fig. 9), which
446 represented heavy pollution days especially happened in winter. The x-axis values of
447 scores significantly decreased year by year. Especially after 2017, the number of high
448 values points gradually decreased with a reduction in x-axis value. The data points in
449 2019 were already close to the y-axis with low x-axis values, indicating the significant
450 decrease of heavy pollution days in the whole year and the improvement of air quality
451 in Beijing.

452 **4.2. Impact of emission reduction on air pollutants**

453 The emission reductions in response to intensified control measures greatly affect
454 the ambient air concentrations (Chen et al., 2019a; Cheng et al., 2019b). Fig. 10 shows
455 the variations of SO₂, NO_x, and dust emissions during 2010–2018 in Beijing. The
456 primary emissions of SO₂ and dust decreased especially after 2017, while NO_x
457 emission was still high although the range decreased. With these decreases, the
458 concentrations of SO₂ decreased most, PM_{2.5} and PM₁₀ decreased significantly,
459 especially after the implementation of the Comprehensive Action, while the decreasing
460 range of NO₂ was much less than that of SO₂. SO₂ is mainly emitted from the coal-fired
461 source, while NO₂ from both coal-fired and vehicle sources (Meng et al., 2018). The
462 coal-fired emission control measures were in line with the emission reduction of SO₂
463 but they were not with NO₂. One of the reasons is that NO_x sourced from vehicle
464 emissions were not effectively controlled, mainly due to the less effective control
465 measures on vehicle emissions, such as traffic restrictions (Wang et al., 2019d; Sun et
466 al., 2018; Fontes et al., 2018; Zhang et al., 2020). Meanwhile, the reductions of PM_{2.5}
467 and PM₁₀ were mainly due to the result of coal-fired control measures (Cheng et al.,
468 2019a). Moreover, the decrease of PM₁₀ was less than PM_{2.5}, which was mainly due to
469 the natural sources including the spring dust storms from the desert areas in north and
470 northwest of China (Liu et al., 2014; Li et al., 2017).

471 **4.3. Impact of energy structure variation on air pollutants**

472 The energy support of China mainly relies on fossil fuels, including coal, petroleum,
473 and natural gas. The previous energy structure was dominated by coal, which was
474 mainly due to the small volume and difficult utilization of other energy types, and the
475 costly development of renewable energy (Ji et al., 2019). With continuous air pollution
476 control strategies, the energy consumption structure of Beijing was optimized, with coal
477 consumption decreased 86.8% and natural gas increased 87.9% during 2013–2018 (Fig.
478 11a). Meanwhile, the socio-economic development had a stable growth with a
479 significant increase in the vehicle population, GDP, total energy consumption, and a
480 notable decrease in major air pollutant concentrations (Fig. 11b). Such an optimized
481 energy structure played an important role in the air quality improvement in Beijing
482 especially by the decrease of coal-fired consumption.

483 **4.4. A comparison of air quality in Beijing with other megacities**

484 Beijing's air quality has been gradually improved in recent years, but the current
485 air pollution levels are still severe. Fig. 12 shows the comparison of PM_{2.5} concentration
486 in Beijing with Shanghai, Shenzhen, and other capital cities around the world. The
487 annual average concentration of PM_{2.5} in Beijing is still much higher than in other
488 capital cities of developed countries, such as Washington DC, London, and Wellington,
489 and other Asian cities, such as Tokyo and Seoul. Meanwhile, the PM_{2.5} concentration
490 of Beijing is also higher than in Chinese domestic cities, such as Shanghai and
491 Shenzhen. However, the PM_{2.5} concentration in Beijing is lower than some cities in
492 developing countries, such as Delhi and Kabul. According to the national standard limit
493 for PM_{2.5}, the moderate air quality level set at 75 µg/m³ might be relatively high, only
494 being close to the initial transition standard of the WHO. Many studies have proved
495 that the concentration of PM_{2.5} at 35–75 µg/m³ could still be harmful to the human body
496 (Di et al., 2017). As the stricter environmental regulations have led to low levels of
497 pollution (Wang et al., 2019a), the air quality standard should be upgraded to maintain
498 a better air quality with a safer PM_{2.5} level. Hence, the control of PM_{2.5} should be
499 intensified depending on a stricter standard. Although O₃ has recently become one of

500 the primary pollutants in Beijing (Beijing Ecology and Environment Statement, 2019),
501 the concentration limit of O₃ is almost in accordance with the international standards
502 (Table 3). Thus, O₃ keeps a low over-standard level when compared to PM_{2.5}. Therefore,
503 we should continue to control PM_{2.5} pollution by cutting coal consumption, and
504 strengthen motor vehicle control to mitigate NO₂ and O₃ pollution. The combined
505 control of PM_{2.5} and O₃ is the key for future air pollution control (Xiang et al., 2020).

506 **5. Conclusions**

507 In this study, the air quality improvement under the Clean Air Action and the
508 Comprehensive Action were assessed by the air monitoring data, and the influencing
509 factors including meteorology, pollutant emissions, and energy structure were discussed.

510 (1) The air quality of Beijing had obvious improvements during 2013–2019, with the
511 most increases in good air quality days and the most decreases in hazardous air quality
512 days. The concentration of SO₂ decreased most, followed by CO, PM_{2.5}, PM₁₀, and NO₂
513 in descending order, except O₃ showed a variable increase.

514 (2) The Comprehensive Action has been more effective in reducing heavy pollution
515 days in winter, and largely reduced the concentrations of coal-fired air pollutants in
516 heating seasons. In 2017, PM_{2.5} and PM₁₀ in the heating period were even lower than
517 those in the non-heating period.

518 (3) PM_{2.5}, PM₁₀, SO₂, and CO concentrations were higher in the southern and central
519 urban areas. The high NO₂ regions became more constrained after the Comprehensive
520 Action, mainly due to the reduction of NO_x from coal-fired emissions. However, the
521 O₃ concentrations were higher in the suburb areas than those in the central urban areas.

522 (4) The meteorological normalized values of SO₂ and CO were lower than the
523 observation data during 2013–2016, and after 2017 these values became higher, which
524 indicated beneficial weather conditions in 2017 and afterwards. But the variation
525 pattern was not as consistent with the changes of PM_{2.5}, PM₁₀, NO₂, and O₃, which
526 indicated that the meteorology could not completely explain the difference between the
527 observation and simulation. The decrease of SO₂ and dust emissions achieved a
528 significant decrease in SO₂, PM_{2.5}, and PM₁₀, while NO_x only had a slight decrease to

529 get a less decrease in NO₂. The significant reduction of coal-burning played a dominant
530 role in improving Beijing's air quality.

531 (5) Beijing's air quality management experiences could guide other developing
532 countries in coping with similar air pollution problems.

533 **Acknowledge**

534 This study is supported by the National Natural Science Foundation of China
535 (Grant No. 41175109) and its project for International Cooperation and Exchanges
536 (Grant No. 41571130031), the National Basic Research Program of China (Grant No.
537 2013CB228503), Beijing Municipal Science & Technology Commission (No.
538 Z181100005418015), and the Yueqi Scholar funds of China University of Mining and
539 Technology (Beijing). All authors declare that they have no competing financial
540 interests.

541 **References**

- 542 Beijing Ecology and Environment Statement, 2019. Beijing Municipal Ecology and Environment
543 Bureau.<http://sthjj.beijing.gov.cn/bjhrb/index/xxgk69/sthjlyzgw/1718880/1718881/1718882/1791057/index.html> (accessed 27 April 2020).
- 544
545 Beijing Environment Statement, 2017. Beijing Municipal Ecology and Environment Bureau.
546 <http://sthjj.beijing.gov.cn/bjhrb/resource/cms/2018/05/2018051614522475279.pdf> (accessed 16
547 May 2018).
- 548 BMG (Beijing Municipal Government), 2013. Beijing 2013–2017 Clean Air Action Plan.
549 http://www.beijing.gov.cn/zhengce/zfwj/zfwj/szfwj/201905/t20190523_72673.html (accessed 12
550 September 2013).
- 551 BSY (Beijing Statistical Yearbooks), 2019. Beijing Municipal Bureau Statistics.
552 http://tjj.beijing.gov.cn/tjsj_31433/.
- 553 Cai, S., Wang, Y., Zhao, B., Wang, S., Chang, X., Hao, J., 2017. The impact of the “Air Pollution
554 Prevention and Control Action Plan” on PM_{2.5} concentrations in Jing-Jin-Ji region during 2012–
555 2020. *Science of The Total Environment*. 580, 197–209.
556 <https://doi.org/10.1016/j.scitotenv.2016.11.188>.
- 557 Camacho, J., 2014. Visualizing Big data with Compressed Score Plots: Approach and research
558 challenges. *Chemometrics and Intelligent Laboratory Systems*.135: 110–25.
559 <https://doi.org/10.1016/j.chemolab.2014.04.011>.
- 560 Chang, L., Shao, L., Yang, S., Li, J., Zhang, M., Feng, X., Li, Y., 2019. Study on variation
561 characteristics of PM_{2.5} mass concentrations in Beijing after the action on comprehensive control of
562 air pollution. *Journal of Mining Science and Technology*. 4(6):539–546. 10.19606/j.cnki.jmst.
563 2019.06.009.
- 564 Chen, L., Guo, B., Huang, J., He, J., Wang, H., Zhang, S., Chen, S.X., 2018a. Assessing air-quality
565 in Beijing-Tianjin-Hebei region: The method and mixed tales of PM_{2.5} and O₃. *Atmospheric*

566 Environment. 193, 290–301. 10.1016/j.atmosenv.2018.08.047.

567 Chen, Z., Xie, X., Cai, J., Chen, D., Gao, B., He, B., Cheng, N., Xu, B., 2018b. Understanding
568 meteorological influences on PM_{2.5} concentrations across China: a temporal and spatial perspective.
569 Atmospheric chemistry and physics. 18, 5343–58. <https://doi.org/10.5194/acp-18-5343-2018>.

570 Chen, Z., Cai, J., Gao, B., Xu, B., Dai, S., He, B., Xie, X., 2017. Detecting the causality influence
571 of individual meteorological factors on local PM_{2.5} concentration in the Jing-Jin-Ji region. Scientific
572 Reports. 7(1): 40735. 10.1038/srep40735.

573 Chen, Z., Chen, D., Kwan, M., Chen, B., Gao, B., Zhuang, Y., Li, R., Xu, B., 2019a. The control of
574 anthropogenic emissions contributed to 80% of the decrease in PM_{2.5} concentrations in Beijing from
575 2013 to 2017. Atmospheric Chemistry and Physics. 19(21), 13519–13533.
576 <https://doi.org/10.5194/acp-19-13519-2019>.

577 Chen, Z., Chen, D., Xie, X., Cai, J., Zhuang, Y., Cheng, N., He, B., Gao, B., 2019b. Spatial self-
578 aggregation effects and national division of city-level PM_{2.5} concentrations in China based on
579 spatio-temporal clustering. Journal of Cleaner Production. 207:875–81.
580 10.1016/j.jclepro.2018.10.080.

581 Cheng, J., Su, J., Cui, T., Li, X., Dong, X., Sun, F., Yang, Y., Tong, D., Zheng, Y., Li, Y., Li, J., Zhang,
582 Q., He, H., 2019a. Dominant role of emission reduction in PM_{2.5} air quality improvement in Beijing
583 during 2013–2017: a model-based decomposition analysis. Atmospheric Chemistry and Physics. 19,
584 6125–6146. <https://doi.org/10.5194/acp-19-6125-2019>.

585 Cheng, N., Cheng, B., Li, S., Ning, T., 2019b. Effects of meteorology and emission reduction
586 measures on air pollution in Beijing during heating seasons. Atmospheric Pollution Research. 10(3):
587 971–9. <https://doi.org/10.1016/j.apr.2019.01.005>.

588 Cobourn, W.G., 2010. An enhanced PM_{2.5} air quality forecast model based on nonlinear regression
589 and back-trajectory concentrations. Atmospheric Environment. 44, 3015–3023.
590 <https://doi.org/10.1016/j.atmosenv.2010.05.009>.

591 Cui, J., Lang, J., Chen, T., Mao, S., Cheng, S., Wang, Z., Cheng, N., 2019. A framework for
592 investigating the air quality variation characteristics based on the monitoring data: Case study for
593 Beijing during 2013–2016. Journal of Environmental Sciences. 81, 225–237.
594 <https://doi.org/10.1016/j.jes.2019.01.009>.

595 Di, Q., Wang, Y., Zanobetti, A., Wang, Y., Koutrakis, P., Choirat, C., Dominici, F., Schwartz, J.D.,
596 2017. Air Pollution and Mortality in the Medicare Population. N Engl J Med. 376, 2513–2522.
597 10.1056/NEJMoal702747.

598 Feng, Y., Ning, M., Lei, Y., Sun, Y., Liu, W., Wang, J., 2019. Defending blue sky in China:
599 Effectiveness of the “Air Pollution Prevention and Control Action Plan” on air quality
600 improvements from 2013 to 2017. Journal of Environmental Management. 252:109603.
601 <https://doi.org/10.1016/j.jenvman.2019.109603>.

602 Fontes, T., Li, P., Barros, N., Zhao, P., 2018. A proposed methodology for impact assessment of air
603 quality traffic-related measures: The case of PM_{2.5} in Beijing. Environmental Pollution. 239, 818–
604 828. <https://doi.org/10.1016/j.envpol.2018.04.061>.

605 Geng, G., Xiao, Q., Zheng, Y., Tong, D., Zhang, Y., Zhang, X., Zhang, Q., He, H., Liu, Y., 2019.
606 Impact of China’s Air Pollution Prevention and Control Action Plan on PM_{2.5} chemical composition
607 over eastern China. Science China (Earth Sciences). 62(12): 1872–84.
608 <https://doi.org/10.1007/s11430-018-9353-x>.

609 Hu, H., Hu, Z., Zhong, K., Xu, J., Zhang, F., Zhao, Y., Wu, P., 2019. Satellite-based high-resolution

610 mapping of ground-level PM_{2.5} concentrations over East China using a spatiotemporal regression
611 kriging model. *Science of The Total Environment*. 672: 479–90.
612 <https://doi.org/10.1016/j.scitotenv.2019.03.480>.

613 Huang, J., Pan, X., Guo, X., Li, G., 2018. Health impact of China's Air Pollution Prevention and
614 Control Action Plan: an analysis of national air quality monitoring and mortality data. *The Lancet*
615 *Planetary Health*. 2(7), e313–e323. [https://doi.org/10.1016/S2542-5196\(18\)30141-4](https://doi.org/10.1016/S2542-5196(18)30141-4).

616 Huang, R.-J., Zhang, Y., Bozzetti, C., Ho, K.-F., Cao, J.-J., Han, Y., Daellenbach, K.R., Slowik, J.G.,
617 Platt, S.M., Canonaco, F., Zotter, P., Wolf, R., Pieber, S.M., Bruns, E.A., Crippa, M., Ciarelli, G.,
618 Piazzalunga, A., Schwikowski, M., Abbaszade, G., Schnelle-Kreis, J., Zimmermann, R., An, Z.,
619 Szidat, S., Baltensperger, U., Haddad, I.E., Prévôt, A.S.H., 2014. High secondary aerosol
620 contribution to particulate pollution during haze events in China. *Nature*. 514, 218–222.
621 <https://doi.org/10.1038/nature13774>.

622 Ji, Q., Zhang, D.. 2019. How much does financial development contribute to renewable energy
623 growth and upgrading of energy structure in China? *Energy Policy*. 128, 114–124.
624 <https://doi.org/10.1016/j.enpol.2018.12.047>.

625 Jin, Y., Andersson, H., Zhang, S., 2016. Air pollution control policies in China: a retrospective and
626 prospects. *International Journal of Environmental Research and Public Health*. 13 (12), 1219.
627 <https://doi.org/10.3390/ijerph13121219>.

628 Li, D., Liu, J., Zhang, J., Gui, H., Du, P., Yu, T., Wang, J., Lu, Y., Liu, W., Cheng, Y., 2017.
629 Identification of long-range transport pathways and potential sources of PM_{2.5} and PM₁₀ in Beijing
630 from 2014 to 2015. *Journal of Environmental Sciences*. 56, 214–229.
631 <https://doi.org/10.1016/j.jes.2016.06.035>.

632 Li, J., Han, X., Jin, M., Zhang, X., Wang, S., 2019a. Globally analysing spatiotemporal trends of
633 anthropogenic PM_{2.5} concentration and population's PM_{2.5} exposure from 1998 to 2016.
634 *Environment International*. 128, 46–62. <https://doi.org/10.1016/j.envint.2019.04.026>.

635 Li, H., You, S., Zhang, H., Zheng, W., Lee, W.-l., Ye, T., Zou, L., 2018. Analyzing the impact of
636 heating emissions on air quality index based on principal component regression. *Journal of Cleaner*
637 *Production*. 171: 1577–92. <https://doi.org/10.1016/j.jclepro.2017.10.106>.

638 Li, R., Li, Z., Gao, W., Ding, W., Xu, Q., Song, X., 2015. Diurnal, seasonal, and spatial variation of
639 PM_{2.5} in Beijing. *Science Bulletin* 60, 387–395. <https://doi.org/10.1007/s11434-014-0607-9>.

640 Li, Y., Shao, L., Wang, W., Zhang, M., Feng, X., Li, W., Zhang, D., 2019b. Airborne fiber particles:
641 Types, size and concentration observed in Beijing. *Science of The Total Environment*
642 2019,705:135967. [10.1016/j.scitotenv.2019.135967](https://doi.org/10.1016/j.scitotenv.2019.135967).

643 Liang, X., Li, S., Zhang, S., Huang, H., Chen, S., 2016. PM_{2.5} Data Reliability, Consistency and Air
644 Quality Assessment in Five Chinese Cities. *Journal of Geophysical Research: Atmospheres*. 121(17):
645 10,220–10,36. <https://doi.org/10.1002/2016JD024877>.

646 Liu, Q., Liu, Y., Yin, J., Zhang, M., Zhang, T., 2014. Chemical characteristics and source
647 apportionment of PM₁₀ during Asian dust storm and non-dust storm days in Beijing. *Atmospheric*
648 *Environment*. 91, 85–94. <https://doi.org/10.1016/j.atmosenv.2014.03.057>.

649 Liu, S., Xing, J., Wang, S., Ding, D., Chen, L., Hao, J., 2020. Revealing the impacts of
650 transboundary pollution on PM_{2.5}-related deaths in China. *Environment International*. 134:105323.
651 <https://doi.org/10.1016/j.envint.2019.105323>.

652 Liu, Z., Xie, M., Tian, K., Gao, P., 2017. GIS-based analysis of population exposure to PM_{2.5} air
653 pollution—A case study of Beijing. *Journal of Environmental Sciences*. 59: 48–53.

654 <https://doi.org/10.1016/j.jes.2017.02.013>.

655 Ma, Q., Wu, Y., Zhang, D., Wang, X., Xia, Y., Liu, X., Tian, P., Han, Z., Xia, X., Wang, Y., Zhang,
656 R., 2017. Roles of regional transport and heterogeneous reactions in the PM_{2.5} increase during winter
657 haze episodes in Beijing. *Science of The Total Environment*. 599–600, 246–253.
658 [10.1016/j.scitotenv.2017.04.193](https://doi.org/10.1016/j.scitotenv.2017.04.193).

659 Maji, K.J., Ye, W.-F., Arora, M., Nagendra, S.M.S., 2019. Ozone pollution in Chinese cities:
660 Assessment of seasonal variation, health effects and economic burden. *Environmental Pollution*.
661 247, 792–801. <https://doi.org/10.1016/j.envpol.2019.01.049>.

662 Meng, K., Xu, X., Cheng, X., Xu, X., Qu, X., Zhu, W., Ma, C., Yang, Y., Zhao, Y., 2018. Spatio-
663 temporal variations in SO₂ and NO₂ emissions caused by heating over the Beijing-Tianjin-Hebei
664 Region constrained by an adaptive nudging method with OMI data. *Science of The Total
665 Environment*. 642, 543–552. <https://doi.org/10.1016/j.scitotenv.2018.06.021>.

666 MEP (Ministry of Ecology and Environment of the People's Republic of China), 2017. Action Plan
667 for Comprehensive Control of Atmospheric Pollution in Autumn and Winter of Beijing-Tianjin-
668 Hebei region in 2017–2018. http://www.mee.gov.cn/gkml/hbb/bwj/201708/t20170824_420330.htm
669 (accessed 21 August 2017).

670 Nguyen, G.T.H., Shimadera, H., Uranishi, K., Matsuo, T., Kondo, A., 2019. Numerical assessment
671 of PM_{2.5} and O₃ air quality in Continental Southeast Asia: Impacts of potential future climate change.
672 *Atmospheric Environment*. 2019, 215: 116901. <https://doi.org/10.1016/j.atmosenv.2019.116901>.

673 Qiu, X., Duan, L., Cai, S., Yu, Q., Wang, S., Chai, F., Gao, J., Li, Y., Xu, Z., 2017. Effect of current
674 emission abatement strategies on air quality improvement in China: A case study of Baotou, a typical
675 industrial city in Inner Mongolia. *Journal of Environmental Sciences*. 57: 383–90.
676 <http://dx.doi.org/10.1016/j.jes.2016.12.014>.

677 Salim, I., Sajjad, R.U., Paule-Mercado, M.C., Memon, S.A., Lee, B.-Y., Sukhbaatar, C., Lee, C.-H.,
678 2019. Comparison of two receptor models PCA-MLR and PMF for source identification and
679 apportionment of pollution carried by runoff from catchment and sub-watershed areas with mixed
680 land cover in South Korea. *Science of The Total Environment*. 663: 764–75.
681 <https://doi.org/10.1016/j.scitotenv.2019.01.377>.

682 Sheehan, M.C., Lam, J., Navas-Acien, A., Chang, H.H., 2016. Ambient air pollution epidemiology
683 systematic review and meta-analysis: A review of reporting and methods practice. *Environment
684 International*. 92–93, 647–656. <https://doi.org/10.1016/j.envint.2016.02.016>.

685 Sun, C., Luo, Y., Li, J., 2018. Urban traffic infrastructure investment and air pollution: Evidence
686 from the 83 cities in China. *Journal of Cleaner Production*. 172, 488–496.
687 <https://doi.org/10.1016/j.jclepro.2017.10.194>.

688 Tan, K.C., San Lim, H., Jafri, M.Z.M., 2016. Prediction of column ozone concentrations using
689 multiple regression analysis and principal component analysis techniques: A case study in
690 peninsular Malaysia. *Atmospheric Pollution Research*. 7(3): 533–46.
691 <https://doi.org/10.1016/j.apr.2016.01.002>.

692 Tao, W., Xue, L., Brimblecombe, P., Lam, Y., Li, L., Zhang, L., 2016. Ozone pollution in China: A
693 review of concentrations, meteorological influences, chemical precursors, and effects. *Science of
694 The Total Environment*. 575. <https://doi.org/10.1016/j.scitotenv.2016.10.081>.

695 The State Council of China, 2013. Air Pollution Prevention and Control Action Plan.
696 http://www.gov.cn/zwqk/2013-09/12/content_2486773.htm (accessed 12 September 2013).

697 Tian, Y., Jiang, Y., Liu, Q., Xu, D., Zhao, S., He, L., Liu, H., Xu, H., 2019. Temporal and spatial

698 trends in air quality in Beijing. *Landscape and Urban Planning*. 185, 35–43.
699 <https://doi.org/10.1016/j.landurbplan.2019.01.006>.

700 UN Environment 2019. A Review of 20 Years' Air Pollution Control in Beijing. United Nations
701 Environment Programme. Nairobi, Kenya.

702 Vu, T.V., Shi, Z., Cheng, J., Zhang, Q., He, K., Wang, S., Harrison, R.M., 2019. Assessing the impact
703 of Clean Air Action Plan on Air Quality Trends in Beijing Megacity using a machine learning
704 technique. *Atmospheric Chemistry and Physics Discussions*. 19(17): 11303–14.
705 <https://doi.org/10.5194/acp-19-11303-2019>.

706 Wang, K., Yin, H., Chen, Y., 2019a. The effect of environmental regulation on air quality: A study
707 of new ambient air quality standards in China. *Journal of Cleaner Production*. 215: 268–79.
708 <https://doi.org/10.1016/j.jclepro.2019.01.061>.

709 Wang, N., Lyu, X., Deng, X., Huang, X., Jiang, F., Ding, A., 2019b. Aggravating O₃ pollution due
710 to NO_x emission control in eastern China. *Science of The Total Environment*. 677, 732–744.
711 <https://doi.org/10.1016/j.scitotenv.2019.04.388>.

712 Wang, W., Chai, F., Zhang, K., Wang, S., Chen, Y., Wang, X., Yang, Y., 2008. Study on ambient air
713 quality in Beijing for the summer 2008 Olympic Games. *Air Quality Atmosphere & Health*. 1(1):
714 31–36. 10.1007/s11869-008-0003-1.

715 Wang, W., Shao, L., Li, J., Chang, L., Zhang, D., Zhang, C., Jiang, J., 2019c. Characteristics of
716 individual particles emitted from an experimental burning chamber with coal from the lung cancer
717 area of Xuanwei, China. *Aerosol and Air Quality Research*. 19, 355–363.
718 10.4209/aaqr.2018.05.0187.

719 Wang, X., Shen, X., Sun, J., Zhang, X., Wang, Y., Zhang, Y., Wang, P., Xia, C., Qi, X., Zhong, J.,
720 2018a. Size-resolved hygroscopic behavior of atmospheric aerosols during heavy aerosol pollution
721 episodes in Beijing in December 2016. *Atmospheric Environment*. 194: 188–97.
722 10.1016/j.atmosenv.2018.09.041.

723 Wang, Y., Li, W., Gao, W., Liu, Z., Tian, S., Shen, R., Ji, D., Wang, S., Wang, L., Tao, S., Cheng,
724 M., Wang, G., Gong, Z., Hao, J., Zhang, Y., 2019d. Trends in particulate matter and its chemical
725 compositions in China from 2013–2017. *Science China Earth Sciences*. 10.1007/s11430-018-9373-
726 1.

727 Wang, Y., Wang, Y., Tang, G., Song, T., Zhou, P., Liu, Z., Hu, B., Ji, D., Wang, L., Zhu, X., Yan, C.,
728 Ehn, M., Gao, W., Pan, Y., Xin, J., Sun, Y., Kerminen, V-M., Kulmala, M., and Petäjä, T., 2018b.
729 Rapid formation of intense haze episode in Beijing. *Atmospheric Chemistry & Physics Discussions*.
730 1–18. <https://doi.org/10.5194/acp-2018-1079>.

731 Wang, Z., Li, Y., Chen, T., Zhang, D., Sun, F., Sun, R., Dong, X., Sun, N., Pan, L. (2014). Temporal
732 and Spatial Distribution Characteristics of Ozone in Beijing. *Environmental Science*. 35(12): 4446–
733 53. 10.13227/j.hjkx.2014.12.005.

734 Wang, Z., Zhang, D., Li, Y., Feng, P., Dong, X., Sun, R., Pan, L., 2015. Analysis of air quality in
735 Beijing city during Spring Festival period of 2014. *Acta Scientiae Circumstantiae*. 35(2): 371–378.
736 10.13671/j.hjkxxb.2014.0798.

737 WHO report. Air pollution data of WHO. <http://apps.who.int/gho/data/node.main.152?lang=en>
738 (accessed 16 May 2018).

739 Wu, J., Yao, F., Li, W., Si, M., 2016. VIIRS-based remote sensing estimation of ground-level PM_{2.5}
740 concentrations in Beijing–Tianjin–Hebei: A spatiotemporal statistical model. *Remote Sensing of*
741 *Environment*. 184, 316–328. <https://doi.org/10.1016/j.rse.2016.07.015>.

742 Xiang, S., Liu, J., Tao, W., Yi, K., Xu, J., Hu, X., Liu, H., Wang, Y., Zhang, Y., Yang, H., Hu, J.,
743 Wan, Y., Wang, X., Ma, J., Wang, X., Tao, S., 2020. Control of both PM_{2.5} and O₃ in Beijing-Tianjin-
744 Hebei and the surrounding areas. *Atmospheric Environment*. 224: 117259.
745 <https://doi.org/10.1016/j.atmosenv.2020.117259>.

746 Xu, S., Ge, J., 2020. Sustainable shifting from coal to gas in North China: An analysis of resident
747 satisfaction. *Energy Policy*. 138: 111296. <https://doi.org/10.1016/j.enpol.2020.111296>.

748 Xu, X., Jiang, Z., Li, J., Chu, Y., Tan, W., Li, C., 2020. Impacts of meteorology and emission control
749 on the abnormally low particulate matter concentration observed during the winter of 2017.
750 *Atmospheric Environment*. 225: 117377. <https://doi.org/10.1016/j.atmosenv.2020.117377>.

751 Xu, X., Zhang, T., 2020. Spatial-temporal variability of PM_{2.5} air quality in Beijing, China during
752 2013–2018. *Journal of Environmental Management*. 262: 110263.
753 <https://doi.org/10.1016/j.jenvman.2020.110263>.

754 Xue, T., Liu, J., Zhang, Q., Geng, G., Zheng, Y., Tong, D., Liu, Z., Guan, D., Bo, Y., Zhu, T., He, K.,
755 Hao, J., 2019. Rapid improvement of PM_{2.5} pollution and associated health benefits in China during
756 2013–2017. *Science China(Earth Sciences)*. 62(12): 1847–56. [https://doi.org/10.1007/s11430-018-](https://doi.org/10.1007/s11430-018-9348-2)
757 [9348-2](https://doi.org/10.1007/s11430-018-9348-2).

758 Yang, X., Liu, S., Shao, P., He, J., Liang, Y., Zhang, B., Liu, B., Liu, Y., Tang, G., Ji, D., 2020.
759 Effectively controlling hazardous airborne elements: Insights from continuous hourly observations
760 during the seasons with the most unfavorable meteorological conditions after the implementation of
761 the APPCAP. *Journal of Hazardous Materials*. 387: 121710.
762 <https://doi.org/10.1016/j.jhazmat.2019.121710>.

763 Zhan, D., Kwan, M-P., Zhang, W., Yu, X., Meng, B., Liu, Q., 2018. The driving factors of air quality
764 index in China. *Journal of Cleaner Production*. 197: 1342–51. [10.1016/j.jclepro.2018.06.108](https://doi.org/10.1016/j.jclepro.2018.06.108).

765 Zhang, H., Cheng, S., Li, J., Yao, S., Wang, X., 2019a. Investigating the aerosol mass and chemical
766 components characteristics and feedback effects on the meteorological factors in the Beijing-
767 Tianjin-Hebei region, China. *Environmental Pollution*. 244, 495–502.
768 <https://doi.org/10.1016/j.envpol.2018.10.087>.

769 Zhang, H., Wang, S., Hao, J., Wang, X., Wang, S., Chai, F., Li, M., 2016. Air pollution and control
770 action in Beijing. *Journal of Cleaner Production*. 112, 1519–1527.
771 <https://doi.org/10.1016/j.jclepro.2015.04.092>.

772 Zhang, M., Shan, C., Wang, W., Pang, J., Guo, S., 2020. Do driving restrictions improve air quality:
773 Take Beijing-Tianjin for example? *Science of The Total Environment*. 712: 136408.
774 <https://doi.org/10.1016/j.scitotenv.2019.136408>.

775 Zhang, Q., Ma, Q., Zhao, B., Liu, X., Wang, Y., Jia, B., Zhang, X., 2018. Winter haze over North
776 China Plain from 2009 to 2016: Influence of emission and meteorology. *Environmental Pollution*.
777 242:1308–18. [10.1016/j.envpol.2018.08.019](https://doi.org/10.1016/j.envpol.2018.08.019).

778 Zhang, Q., Zheng, Y., Tong, D., Shao, M., Wang, S., Zhang, Y., Xu, X., Wang, J., He, H., Liu, W.,
779 Ding, Y., Lei, Y., Li, J., Wang, Z., Zhang, X., Wang, Y., Cheng, J., Liu, Y., Shi, Q., Yan, L., Geng,
780 G., Hong, C., Li, M., Liu, F., Zheng, B., Cao, J., Ding, A., Gao, J., Fu, Q., Huo, J., Liu, B., Liu, Z.,
781 Yang, F., He, K., 2019b. Drivers of improved PM_{2.5} air quality in China from 2013 to 2017.
782 *Proceedings of the National Academy of Sciences*. 116:201907956. [10.1073/pnas.1907956116](https://doi.org/10.1073/pnas.1907956116).

783 Zhang, S., Guo, B., Dong, A., He, J., Xu, Z., Chen, S., 2017. Cautionary tales on air-quality
784 improvement in Beijing. *Proceedings of the Royal Society A: Mathematical, Physical and*
785 *Engineering Science*. 473, 20170457. [10.1098/rspa.2017.0457](https://doi.org/10.1098/rspa.2017.0457).

786 Zhang, X., Xu, X., Ding, Y., Liu, Y., Zhang, H., Wang, Y., Zhong, J., 2019c. The impact of
787 meteorological changes from 2013 to 2017 on PM_{2.5} mass reduction in key regions in China. *Science*
788 *China Earth Sciences*. 62. <https://doi.org/10.1007/s11430-019-9343-3>.
789 Zhang, Y. L., 2019. Dynamic effect analysis of meteorological conditions on air pollution: A case
790 study from Beijing. *Science of The Total Environment*. 684: 178–85.
791 <https://doi.org/10.1016/j.scitotenv.2019.05.360>.
792 Zheng, G., Duan, F., Su, H., Ma, Y., Cheng, Y., Zheng, B., Zhang, Q., Huang, T., Kimoto, T., Chang,
793 D., Pöschl, U., Cheng, Y., He, K., 2015. Exploring the severe winter haze in Beijing: The impact of
794 synoptic weather, regional transport and heterogeneous reactions. *Atmospheric Chemistry and*
795 *Physics*. 15, 2969–2983. 10.5194/acp-15-2969-2015.
796

797

Figures

798 Figure 1 The distribution map of automatic air quality ground monitoring stations in
799 Beijing.

800 Figure 2 The distributions of days under different air quality levels and the annual mean
801 of AQI in Beijing.

802 Figure 3 Time-series of the daily average of AQI in Beijing.

803 Figure 4 Time-series of the daily, monthly, and seasonal concentrations of (a) PM_{2.5}, (b)
804 PM₁₀, (c) SO₂, (d) CO, (e) NO₂, (f) O₃ between January 2013 and February
805 2020 in Beijing.

806 Figure 5 The concentration of PM_{2.5}, PM₁₀, SO₂, NO₂, CO, and O₃ in the heating period
807 and the non-heating period at stage I and stage II in Beijing.

808 Figure 6 Spatial distributions of PM_{2.5}, PM₁₀, SO₂, NO₂, CO, and O₃ in the heating
809 period and the non-heating period at stage I and stage II in Beijing.

810 Figure 7 Comparison of observed (black line) and simulated (red line) monthly average
811 of (1) PM_{2.5}, (2) PM₁₀, (3) SO₂, (4) NO₂, (5) CO, and (6) O₃ in Beijing.

812 Figure 8 Comparison of the stimulated monthly average concentration of PM_{2.5} by
813 PCA-MNLR and WRF-CMAQ (Cheng et al., 2019x).

814 Figure 9 The score plot of PC1 and PC2 by the PCA method.

815 Figure 10 The variations of air pollutant emission during 2010–2018 in Beijing.

816 Figure 11 The variations of (a) energy consumption structure, and (b) socio-economic
817 in Beijing, 2010–2018.

818 Figure 12 The comparison of the annual mean concentration of PM_{2.5} in different capital
819 cities worldwide in 2013 and 2018.

820

Tables

822 Table 1 Sub-index of air pollutants and the corresponding concentration limits of
823 different AQI levels.

824 Table 2 The different levels of AQI values and the corresponding health implications
825 and cautionary statement.

826 Table 3 Air quality standards for air pollutants set by the Chinese government and other
827 countries. Table 4 The major control measures of the Clean Air Action and the
828 Comprehensive Action.

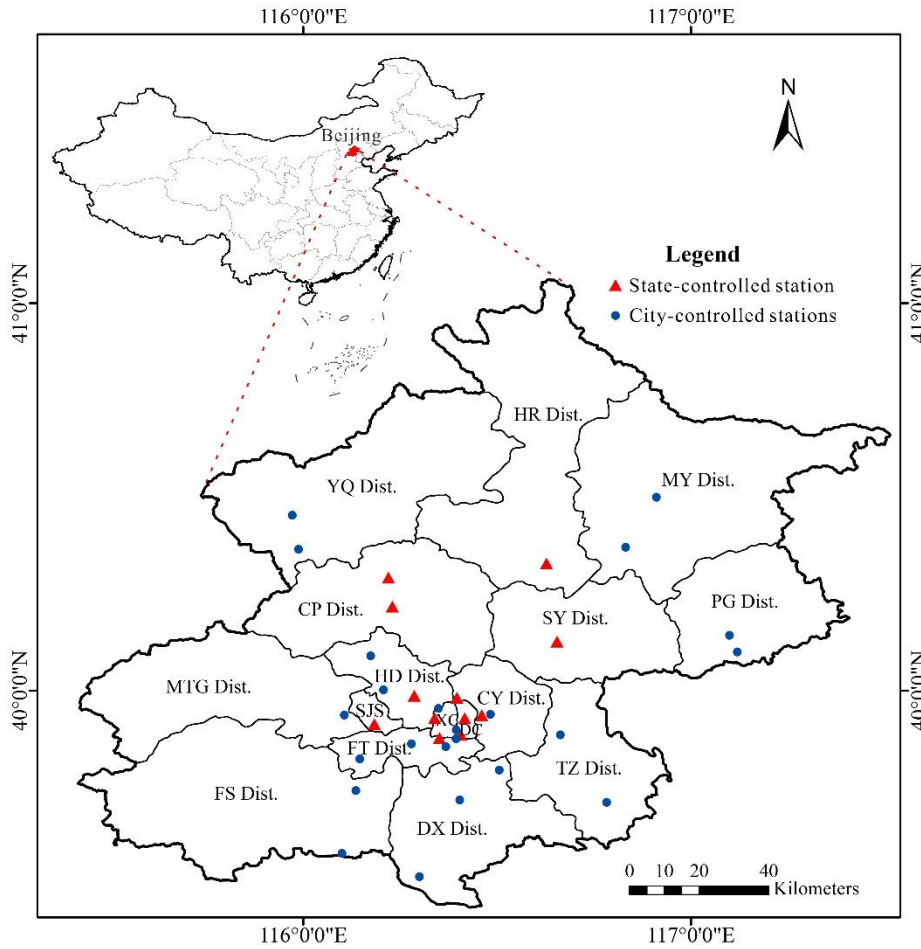
829 Table 5 Annual mean concentration of air pollutants in Beijing.

830 Table 6 A comparison of the annual mean concentrations of air pollutants after the
831 meteorological normalization from this study and other references.

832

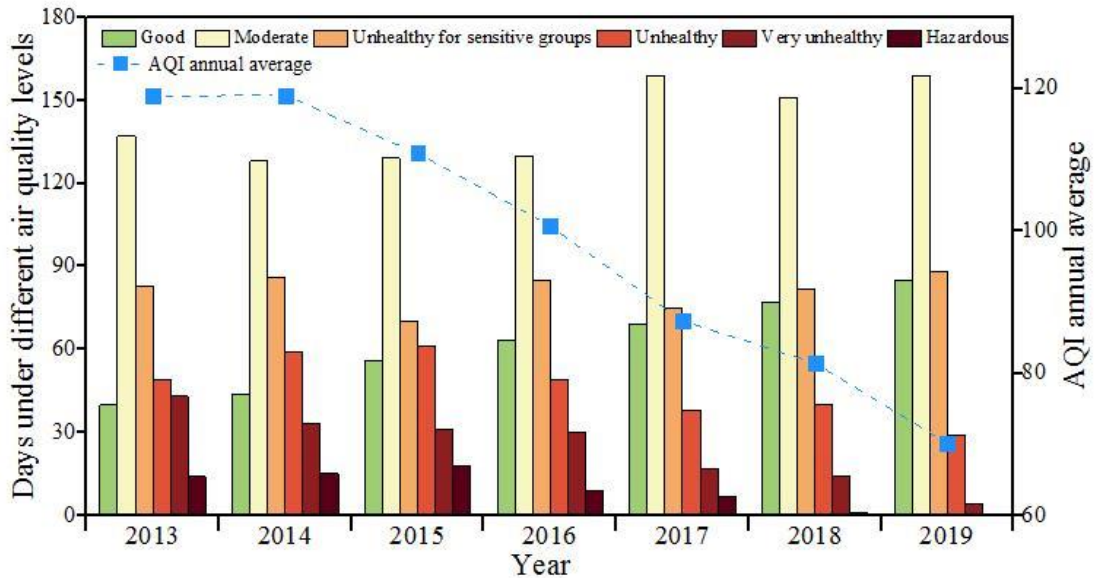
833 Note: Some explanations and descriptions of the above figures and tables were added
834 after their titles. Please see the detailed text below.

835



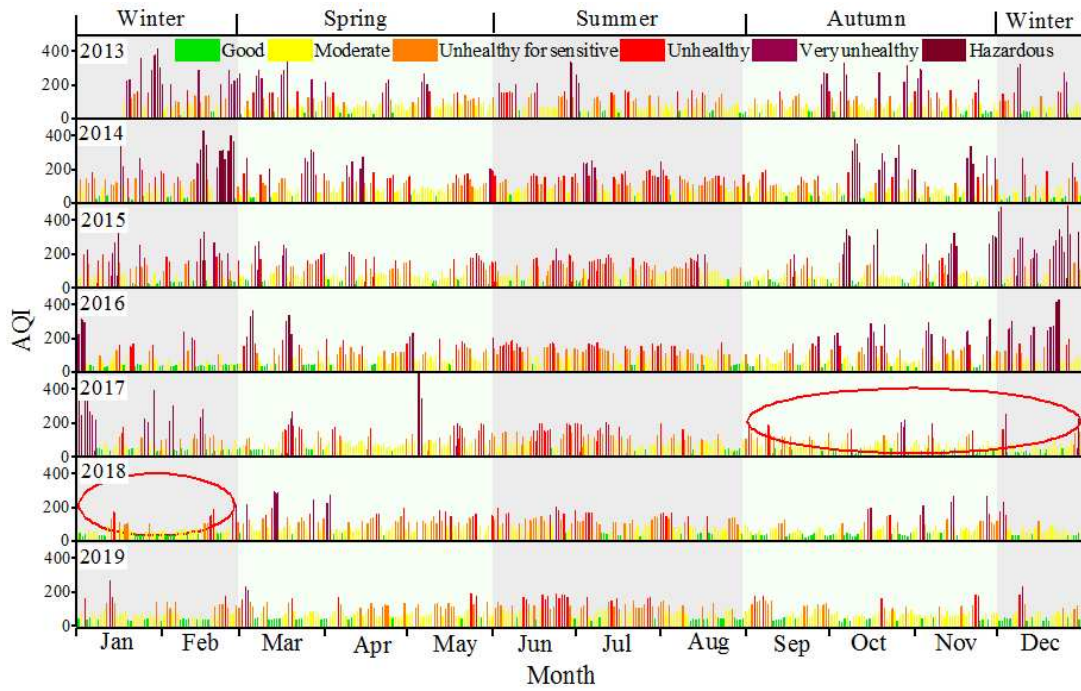
836
837
838

Fig. 1. The distribution map of automatic air quality ground monitoring stations in Beijing.



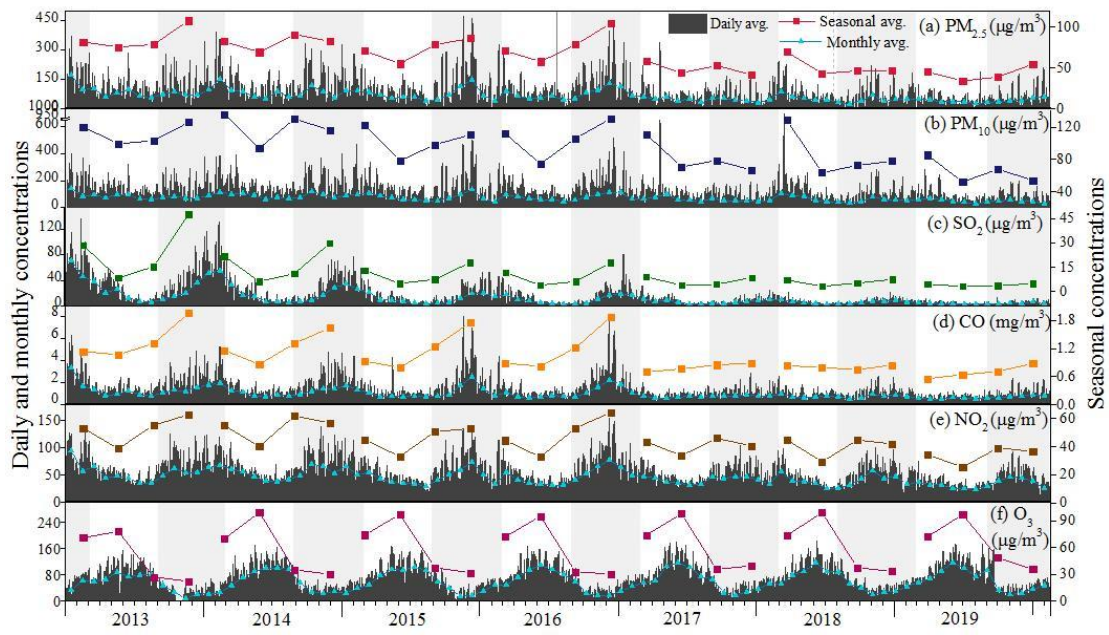
839

840 Fig. 2. The distributions of days under different air quality levels and the annual mean of AQI in
841 Beijing. Meet-standard days include good air quality days and moderate air quality days, and
842 heavy pollution days include very unhealthy days and hazardous days. Note: the annual mean of
843 AQI decreased yearly, good air quality days increased most, and hazardous days decreased most.



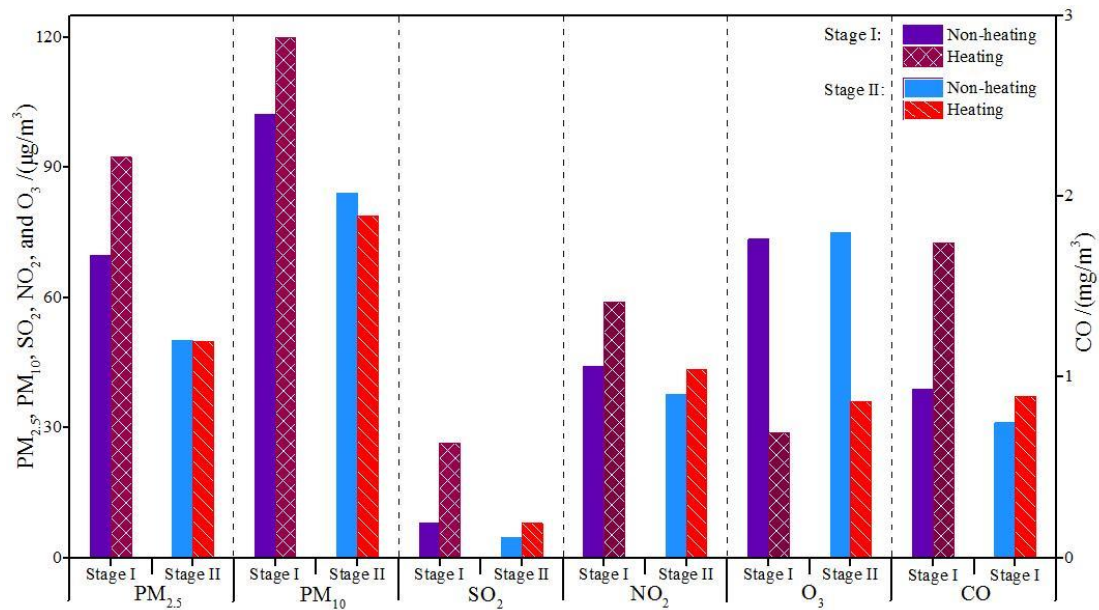
844
845
846
847

Fig. 3. Time-series of the daily average of AQI in Beijing. Please note that the red circled areas refer to autumn and winter in 2017 where the daily values of AQI had a significant decrease.



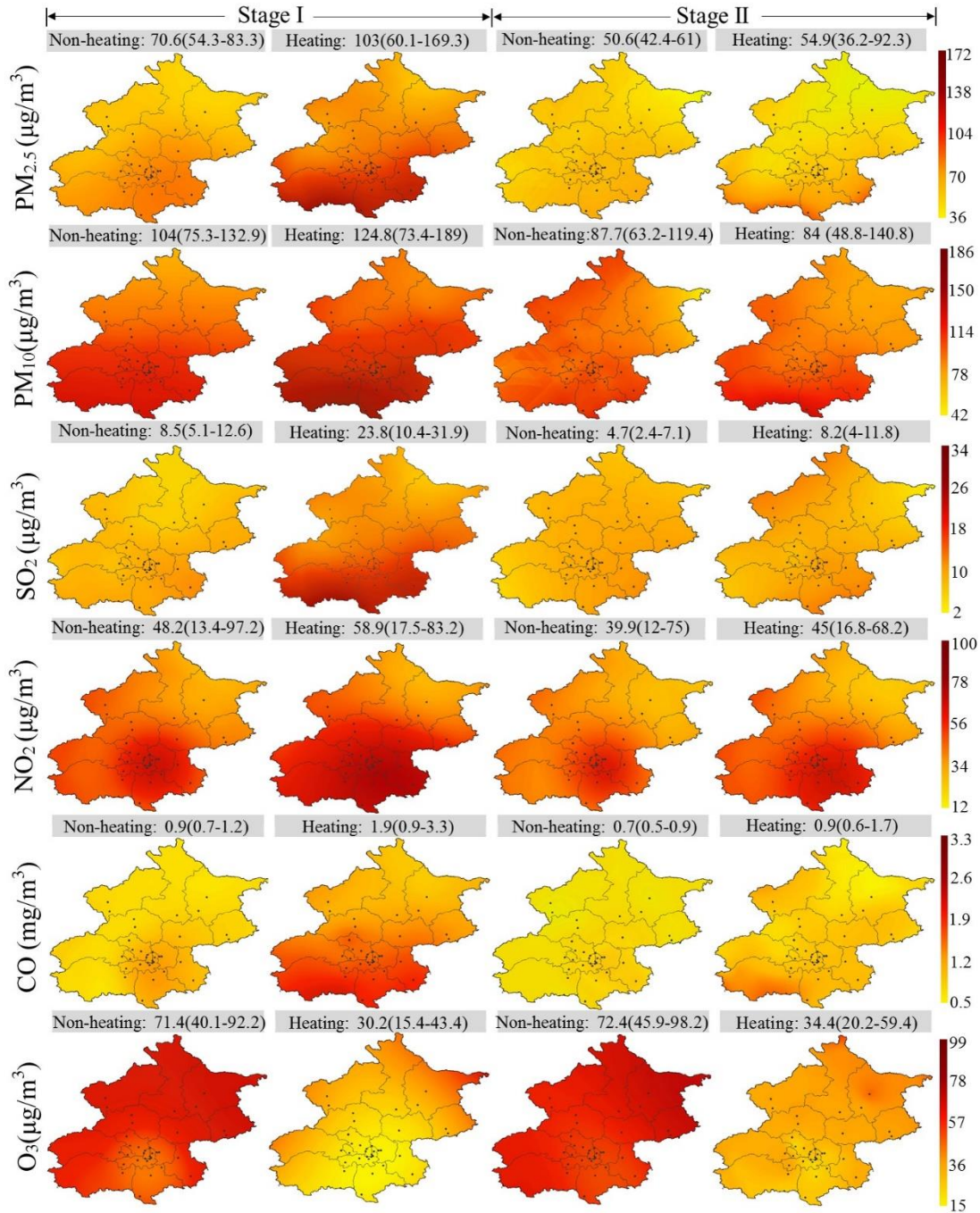
848
849
850
851
852
853
854

Fig. 4. Time-series of the daily, monthly, and seasonal concentrations of (a) $PM_{2.5}$, (b) PM_{10} , (c) SO_2 , (d) CO , (e) NO_2 , (f) O_3 between January 2013 and February 2020 in Beijing. Grey colors in the background refer to autumn (September to November) and winter (December to February), and light colors refer to spring (March to May) and summer (June to August). Note: SO_2 and CO decreased obviously and tended to be flat, and $PM_{2.5}$, PM_{10} , and NO_2 decreased but still fluctuated, while O_3 increased with a different seasonal distribution compared to other pollutants.



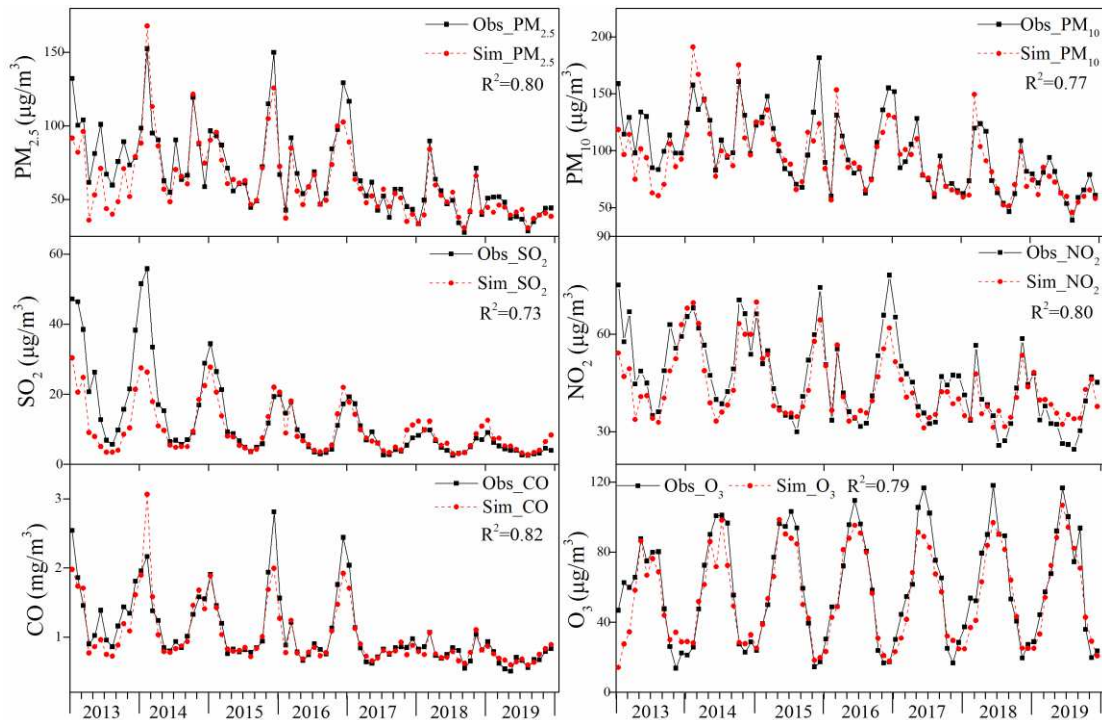
855
856
857
858
859
860
861

Fig. 5. The concentration of PM_{2.5}, PM₁₀, SO₂, NO₂, CO, and O₃ in the heating period and the non-heating period at stage I and stage II in Beijing. The heating period is from November 15 to March 15, and the non-heating period is from March 16 to November 14. Note: At stage I, the air pollutant concentration was higher in the heating period, but at stage II these decreased dramatically, PM_{2.5} and PM₁₀ were lower in the heating period. However, O₃ was increased in both the heating and non-heating period.



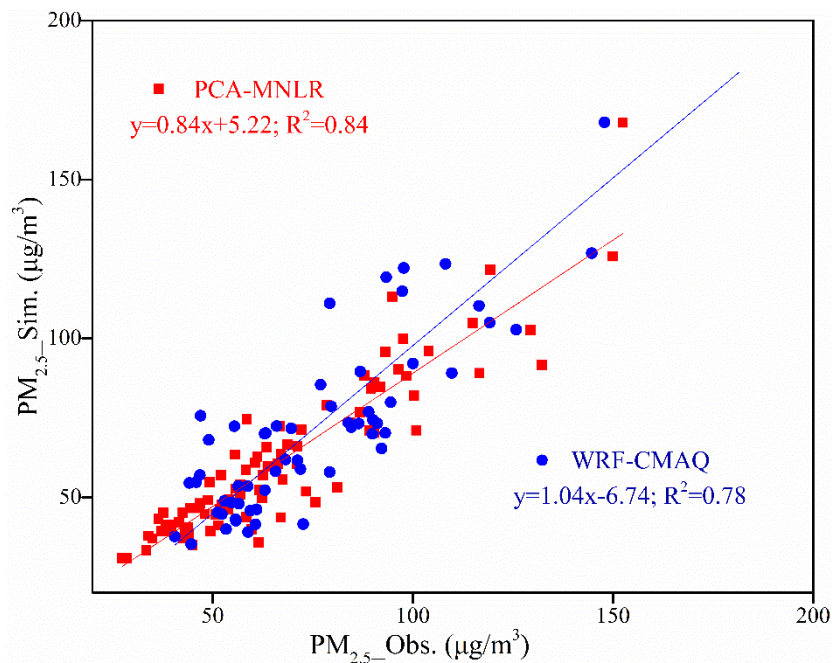
862

863 Fig. 6. Spatial distributions of PM_{2.5}, PM₁₀, SO₂, NO₂, CO, and O₃ in the heating period and the
 864 non-heating period at stage I and stage II in Beijing. The numbers above each picture signify the
 865 average value (outside) and variation range (inside the bracket). Note: air pollutants decreased
 866 significantly in the heating period at stage II. O₃ had a different changing pattern and increased at
 867 stage II. The southern region had a more serious pollution situation.



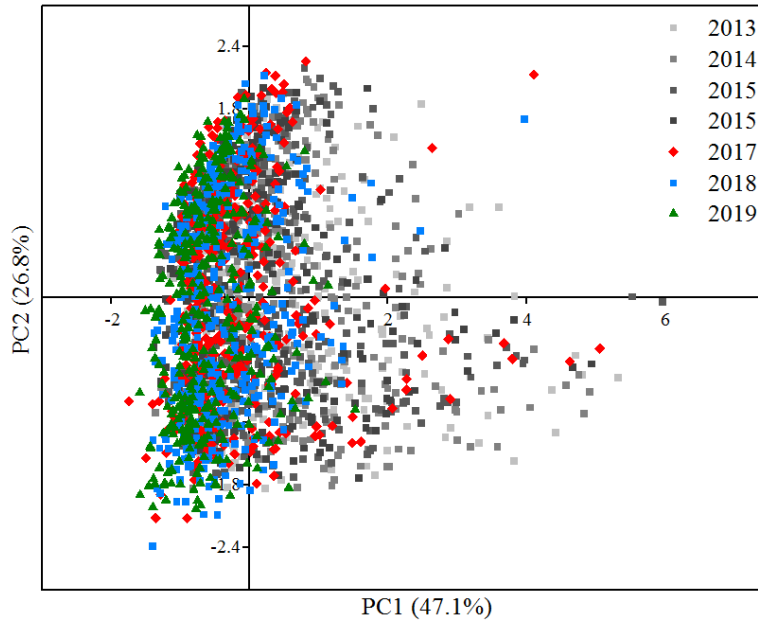
868

869 Fig. 7. Comparison of observed (black line) and simulated (red line) monthly average of (1) PM_{2.5},
 870 (2) PM₁₀, (3) SO₂, (4) NO₂, (5) CO, and (6) O₃ in Beijing. Note: the meteorological normalized
 871 values of major air pollutants were lower during 2013–2016, but these values became higher than
 872 the observed values after 2017, which indicated the more beneficial weather conditions in 2017.
 873



874

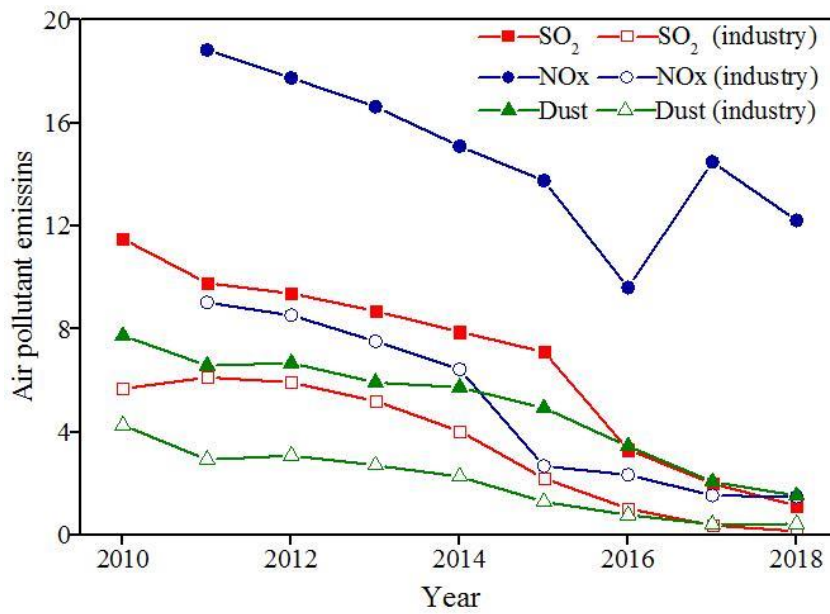
875 Fig. 8. Comparison of the stimulated monthly average concentration of PM_{2.5} by PCA-MNLR
 876 (this study) and WRF-CMAQ (Cheng et al., 2019a).
 877



878

879 Fig. 9. The score plot of PC1 and PC2 by the PCA method. Note: The PCs dots had descending x-
 880 axis values, indicating the significant decrease of heavy pollution days after 2017.

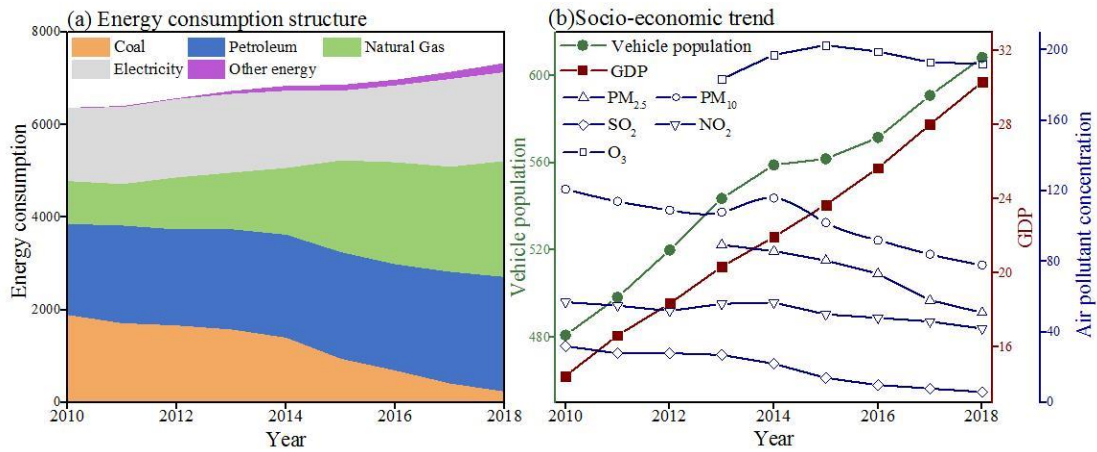
881



882

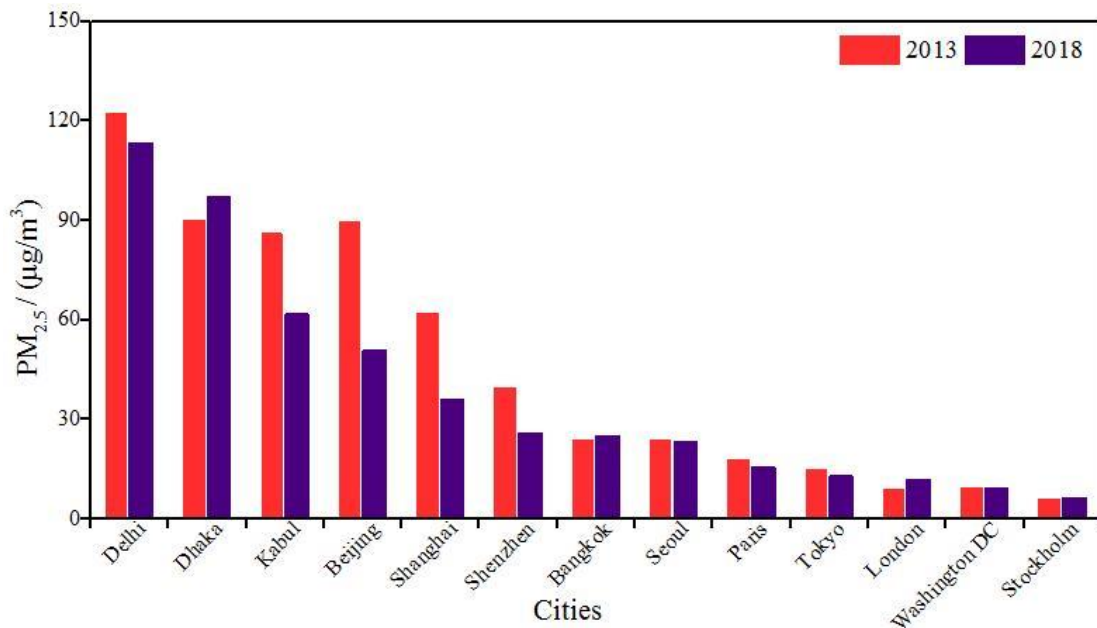
883 Fig. 10. The variations of air pollutant emission during 2010–2018 in Beijing. Data came from the
 884 Beijing Statistical Yearbooks (BSY, 2019). Unit: 10,000 tons. Note: SO₂ and dust emissions
 885 decreased gradually, while NO_x emission had a fluctuant decrease.

886



887
888
889
890
891
892
893

Fig. 11. The variations of (a) energy consumption structure, and (b) socio-economic in Beijing, 2010–2018. Data came from the Beijing Statistical Yearbooks (BSY, 2019). Unit: 10,000 tons of SCE for (a) energy consumption structure; 10,000 units for vehicle population, 100 billion yuan for GDP, $\mu\text{g}/\text{m}^3$ for $\text{PM}_{2.5}$, PM_{10} , SO_2 , NO_2 , and O_3 . Note: Coal consumption decreased significantly, with steady socio-economic growth and gradual air pollutants decrease.



894
895
896
897
898
899
900

Fig. 12. The comparison of the annual mean concentration of $\text{PM}_{2.5}$ in different capital cities worldwide in 2013 and 2018. Data came from a World Health Organization report (WHO Report). Note: $\text{PM}_{2.5}$ of Beijing is still higher than some capital cities of developed countries, some Asian cities, and some domestic cities, and also is lower than some cities of developing countries.

901 **Table 1**

902 Sub-index of air pollutants and the corresponding concentration limits of different AQI levels.

903 Unit: $\mu\text{g}/\text{m}^3$ for all air pollutants, except CO (mg/m^3).

IAQI	PM _{2.5}	PM ₁₀	SO ₂		NO ₂		O ₃		CO	
	24h ¹	24h ¹	24h ¹	1h ²	24h ¹	1h	8h ³	1h	24h ¹	1h
0	0	0	0	0	0	0	0	0	0	0
50	35	50	50	150	40	100	100	160	2	5
100	75	150	150	500	80	200	160	200	4	10
150	115	250	475	650	180	700	215	300	14	35
200	150	350	800	800	280	1200	265	400	24	60
300	250	420	1600	-	565	2340	800	800	36	90
400	350	500	2100	-	750	3090	-	1000	48	120
500	500	600	2620	-	940	3840	-	1200	60	150

904 ¹ the daily average of PM_{2.5}, PM₁₀, SO₂, NO₂, and CO is used in daily evaluation;

905 ² the hourly average of SO₂, NO₂, O₃, and CO is only used in the hourly evaluation. When the
906 hourly average of SO₂ exceeds 800 $\mu\text{g}/\text{m}^3$, the hourly IAQI will not be calculated and the daily
907 concentration should be used instead.

908 ³ when the 8 hour average of O₃ exceeds 800, the 8-hour IAQI will not be calculated and the
909 hourly concentration should be used instead.

910

911 **Table 2**

912 The different levels of AQI values and the corresponding health implications and cautionary
 913 statement.

AQI values	AQI levels	Air quality level	Health implications	Cautionary statement
0–50	I	Good	Air quality is considered satisfactory, and air pollution poses little or no risk.	Everyone can do normal activities.
51–100	II	Moderate	Air quality is acceptable; however, some pollutants may have a moderate health concern for a very small number of people with abnormal sensitivity.	A very small number of people with abnormal sensitivity should limit outdoor exertion.
101–150	III	Unhealthy for sensitive groups	Members of sensitive groups may have a mild increase in symptoms. The general public may experience irritation symptoms.	Children, the elderly, and people with heart and respiratory disease should limit prolonged and intense outdoor exertion.
151–200	IV	Unhealthy	Members of sensitive groups may have further aggravated symptoms. The general public may experience an impact on the heart and respiratory symptoms.	Children, the elderly, and people with heart and respiratory disease should limit prolonged and intense outdoor exertion; everyone else should properly limit outdoor exertion.
201–300	V	Very unhealthy	Patients with heart and lung disease may have significantly increased symptoms and decreased exercise tolerance. The general public may widely experience symptoms.	Children, the elderly, and people with heart and lung disease, should stay indoors and stop outdoor exertion; everyone else should limit outdoor exertion.
>300	VI	Hazardous	The general public may have decreased exercise tolerance and obvious strong symptoms and may have some diseases in advance.	Children, the elderly, and patients should stay indoors and avoid physical exertion; everyone else should avoid outdoor exertion.

914

915

Pollutant	Time	China I ¹	China II ¹	WHO 2006	USA I	USA II	European Union	Japan	South Korea	India	Australia
PM _{2.5} (µg/m ³)	yearly	15	35	10	12	15	25	15	25	40	8
	daily	35	75	25	35	35		35	50	60	25
PM ₁₀ (µg/m ³)	yearly	40	70	20	-	-	40	-	50	60	-
	daily	50	150	50	150	150	50	80	100	100	50
SO ₂ (µg/m ³)	yearly	20	60		-	-		-	0.02 ²	50	0.02 ²
	daily	50	150	20	-	-	125	0.04 ²	0.05 ²	80	0.08 ²
	hourly	150	500	-	75 ²	0.05 ^{3,4}	300	0.1 ²	0.15 ²	-	0.2 ²
NO ₂ (µg/m ³)	yearly	40	40	40	53 ³	53 ³	40	-	0.03 ²	40	0.03 ²
	daily	80	80		-	-		0.04	0.06 ²	80	-
	hourly	200	200	200	100 ³	-	200	-	0.1 ²	-	0.12 ²
CO (mg/m ³)	1 day	4	4	-	-	-	-	10 ²	-	-	-
	8 hours			10	9 ²	-	10	20 ²	9 ²	2	9 ²
	hourly	10	10	30	35 ²	-	-	-	25 ²	4	-
O ₃ (µg/m ³)	8 hours	100	160	100	0.07 ²	0.07 ²	120	-	0.06 ²	100	-
	4 hours			-	-	-	-	-	-	-	0.08 ²
	1 hour	160	200		-	-		60	0.1 ²	180	0.1 ²

918 ¹ China I is the first-level concentration limit of China national ambient air quality standards
919 (NAAQS-I), suitable for the ecologically sensitive areas, tourist attractions, and other areas required
920 special protection. China II is the second-level concentration limit of China national ambient air
921 quality standards (NAAQS-II), suitable for industrial, residential, rural, and other areas.

922 ² units refer to parts per million (ppm).

923 ³ units refer to parts per billion (ppb).

924 ⁴ the average value of 3 hours.

925 data source: China (<http://www.mee.gov.cn/>). USA (<https://www.epa.gov/criteria-air-pollutants>).

927 **Table 4**

928 The major control measures of the Clean Air Action and the Comprehensive Action. A refer to the
 929 Clean Air Action, and B refers to the Comprehensive Action. This classification of pollution
 930 sources is depended on the classification in the source apportionment from Beijing Ecology and
 931 Environmental Statement 2018.

Action	Pollution source	Measures
A	Coal-fired emissions	(1) Adjust and optimize the energy structure.
		(2) Utilize clean coal.
		(3) Increase clean energy alternatives such as coal-to-gas or coal-to-electricity, and increase clean energy sources such as hydropower, wind power, and solar energy.
		(4) Renovate or eliminate coal-fired boilers.
		(5) Improve energy efficiency.
		(6) Eliminate civil bulk coal consumption.
A	Industrial emissions	(1) Adjust industrial structure, optimize the industrial layout, and promote industrial upgrade.
		(2) Rectify polluting businesses and enterprises.
		(3) Eliminate or upgrade industries with excessive, backward, and polluting industries.
		(4) Reduce volatile organic compounds (VOCs) emission.
		(5) Promote cleaner production (CP).
		(6) Accelerate the technological transformation and improve innovation capability.
A	Vehicle emissions	(1) Make strict standards for new vehicles.
		(2) Retrofit in-use vehicles, eliminate "yellow-labeled" vehicles, and retire old vehicles.
		(3) Improve fuel quality and develop new energy vehicles.
		(4) Optimize traffic structure.
A	Dust emissions	(1) Increase the quality and frequency of the road cleaning process.
		(2) Shut down concrete mixing plants and update cinder block transporters.
		(3) Make an afforestation project.
A	Other measures	(1) Improve environmental law, regulation system, and economic policy.
		(2) Enhance atmospheric environmental supervision capability.
		(3) Establish regional coordination mechanisms.
		(4) Monitor emergency response systems to deal with heavy pollution events.
		(5) Mobilize public participation.
B	Coal-fired emission	(1) Partial halt production in the steel industry.
		(2) Full halt production in the building material industries, and optimization of production control in the nonferrous chemical industries.
		(3) Full halted production in the cement powder stations during the heavy pollution emergency period.
	Others	Other measures carried out are according to the "Clean Air Action".

932

933

934 **Table 5**

935 The annual mean concentration of air pollutants in Beijing. Data came from Beijing's ecology and
936 environment statement.

Year	PM _{2.5} ($\mu\text{g}/\text{m}^3$)	PM ₁₀ ($\mu\text{g}/\text{m}^3$)	SO ₂ ($\mu\text{g}/\text{m}^3$)	CO-24h (mg/m^3)	NO ₂ ($\mu\text{g}/\text{m}^3$)	O ₃ -8h ($\mu\text{g}/\text{m}^3$)
2013	89.5	108.1	26.5	3.4	56.0	183.4
2014	85.9	115.8	21.8	3.2	56.7	197.2
2015	80.6	101.5	13.5	3.6	50.0	202.6
2016	72.6	92.0	10.0	3.2	48.0	199.0
2017	58.0	84.0	8.0	2.1	46.0	193.0
2018	51.0	78.0	6.0	1.7	42.0	192.0
2019	42.0	68.0	4.0	1.4	37.0	191.0
NAAQS II	35.0	70.0	60.0	4.0	40.0	160.0

937

938

939 *Supplement of*
940 **Air quality improvement in response to intensified**
941 **control strategies in Beijing during 2013–2019**

942
943
944
945
946
947
948
949
950
951
952
953
954

955 **CONTENTS**

956 **Figures: Figure S1**

957 **Figure S1 The concentration of (a) PM_{2.5}, (b) PM₁₀, (c)SO₂, (d) CO, (e) NO₂, (f) O₃ in**
958 **the heating period and the non-heating period during 2013–2019 in Beijing.**

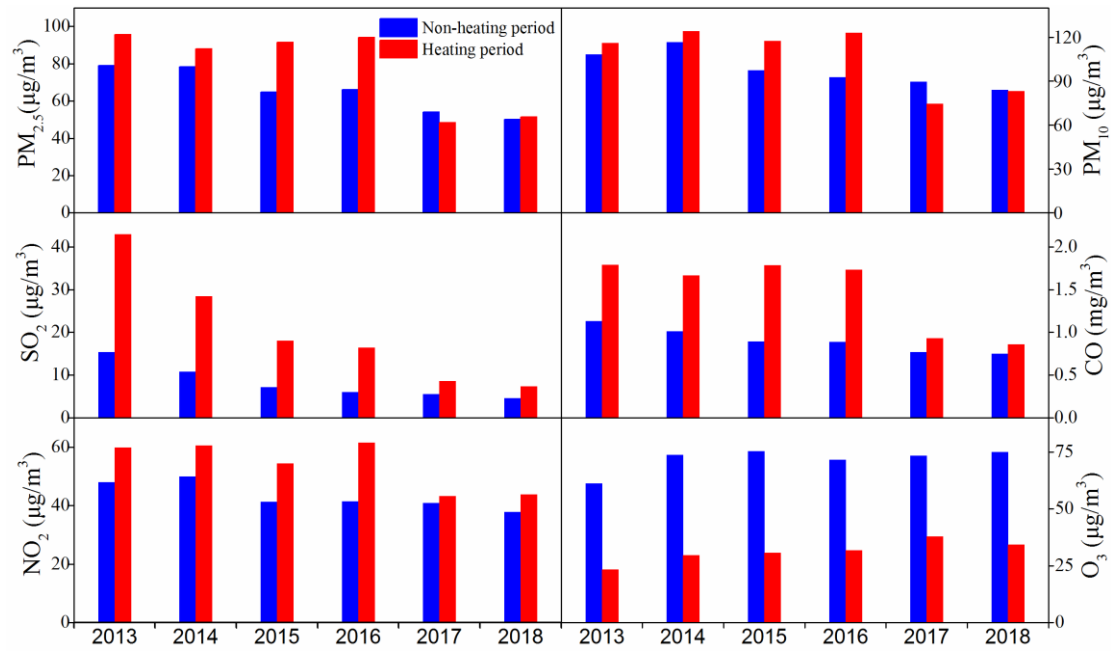
959

960 **Tables: Table S1 to Table S2**

961 **Table S1 The measurement method and instrument of each pollutant.**

962 **Table S2 A comparison of the annual mean concentrations of air pollutants after the**
963 **meteorological normalization from this study and other references.**

964



965
 966
 967
 968
 969
 970
 971

Fig. S1. The concentration of (a) PM_{2.5}, (b) PM₁₀, (c)SO₂, (d) CO, (e) NO₂, (f) O₃ in the heating period and the non-heating period during 2013–2019 in Beijing. Note: The concentrations of pollutants in the heating period decreased yearly, especially after 2017, except O₃. The data of this study included January 2013 to February 2020, which didn't cover the heating period of 2019. For that reason, the heating period and the non-heating period of 2019 were not compare in this figure.

972 **Table S1**

973 The measurement method and instrument of each pollutant. Note: Calibrations were strictly
 974 adhered according to Technical specifications for operation and quality control of ambient air
 975 quality continuous automated monitoring system for SO₂, NO₂, O₃, and CO (HJ 808-2018) and
 976 particulate matter (HJ 817-2018).

Pollutants	Method	Instrument
PM _{2.5}	Tapered element oscillating microbalance (TEOM)	Thermo Fisher 1405F
PM ₁₀	Tapered element oscillating microbalance (TEOM)	Thermo Fisher 1400
SO ₂	Ultraviolet fluorescence method	Thermo Fisher 43i
NO/NO ₂ / NO _x	Chemiluminescence (CL) method	Thermo Fisher 42C
CO	Gas filter infrared absorption method	Thermo Fisher 48C
O ₃	Ultraviolet spectrophotometry method	Thermo Fisher 49C

977

978

979 **Table S2**

980 A comparison of the annual mean concentrations of air pollutants after the meteorological
 981 normalization from this study and other references.

Pollutant	Year	Obs.	Sim.	Others	Pollutant	Year	Obs.	Sim.	Others
PM _{2.5} ($\mu\text{g}/\text{m}^3$)	2013	89.5	80.6	93 ¹ , 86 ²	NO ₂ ($\mu\text{g}/\text{m}^3$)	2013	56.0	54.8	58 ¹ , 63 ²
	2014	85.9	86.8	85 ¹ , 83 ²		2014	56.7	53.2	56 ¹ , 61 ²
	2015	80.6	75.7	75 ¹ , 75 ²		2015	50.0	48.6	50 ¹ , 57 ²
	2016	73.0	68.1	71 ¹ , 70 ²		2016	48.0	46.2	48 ¹ , 56 ²
	2017	58.0	53.1	61 ¹ , 54 ²		2017	46.0	42.7	48 ¹ , 55 ²
	2018	51.0	49.2	-		2018	42.0	39.7	-
	2019	42.0	40.5	-		2019	37.0	36.3	-
PM ₁₀ ($\mu\text{g}/\text{m}^3$)	2013	108.1	113.5	123 ¹ , 124 ²	CO* (mg/m^3)	2013	1.4	1.2	1.5 ¹ , 1.2 ²
	2014	115.8	122.7	121 ¹ , 128 ²		2014	1.3	1.4	1.3 ¹ , 1.2 ²
	2015	101.5	105.5	106 ¹ , 106 ²		2015	1.3	1.2	1.2 ¹ , 1.1 ²
	2016	92.0	95.5	101 ¹ , 103 ²		2016	1.1	1.0	1.1 ¹ , 1.1 ²
	2017	84.0	86.2	93 ¹ , 96 ²		2017	0.9	0.9	1.0 ¹ , 1.1 ²
	2018	78.0	79.5	-		2018	0.8	0.8	-
	2019	68.0	64.8	-		2019	0.7	0.7	-
SO ₂ ($\mu\text{g}/\text{m}^3$)	2013	26.5	20.4	26.3 ¹ , 37 ²	O ₃ * ($\mu\text{g}/\text{m}^3$)	2013	55.6	47.3	59 ¹ , 47 ²
	2014	21.8	18.6	20 ¹ , 28 ²		2014	57.4	53.0	56 ¹ , 46 ²
	2015	13.5	11.6	13 ¹ , 19 ²		2015	59.0	56.2	59 ¹ , 44 ²
	2016	10.0	10.1	10 ¹ , 15 ²		2016	58.1	56.3	60 ¹ , 49 ²
	2017	8.0	8.8	8.4 ¹ , 11 ²		2017	60.4	53.1	61 ¹ , 49 ²
	2018	6.0	7.2	-		2018	62.5	56.2	-
	2019	4.0	5.8	-		2019	62.8	59.9	-

982 ¹ data is from Vu et al. (2019);

983 ² data is from Cheng et al. (2019a);

984 * the annual mean concentration of CO and O₃ is calculated by daily average concentration, which
 985 is different from the official data.